



TECHNICAL REPORT M-74-7

PERFORMANCE EVALUATION OF A SECOND-GENERATION ELASTIC LOOP MOBILITY SYSTEM

by

K.-J. Melzer, G. D. Swanson



(NASA-CR-139531) PERFORMANCE EVALUATION OF A SECOND-GENERATION ELASTIC LOOP MOBILITY SYSTEM FINAL REPORT (ARMY Engineer Waterways Experiment Station) 34 p HC \$7.75

CSC 138 33/11 40217

M74-30603

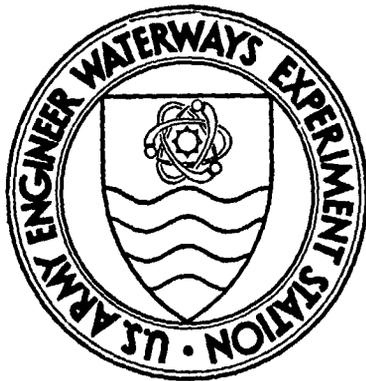
June 1974

Prepared For **George C. Marshall Space Flight Center**
National Aeronautics and Space Administration, Huntsville, Alabama

Conducted by **U. S. Army Engineer Waterways Experiment Station**
Mobility and Environmental Systems Laboratory
Vicksburg, Mississippi

APPROVED FOR PUBLIC RELEASE; DISTRIBUTION UNLIMITED

REPRODUCIBILITY OF THE ORIGINAL PAGE IS POOR



TECHNICAL REPORT M-74-7

PERFORMANCE EVALUATION OF A SECOND-GENERATION ELASTIC LOOP MOBILITY SYSTEM

by

K.-J. Melzer, G. D. Swanson



June 1974

Prepared For **George C. Marshall Space Flight Center**
National Aeronautics and Space Administration, Huntsville, Alabama

Conducted by **U. S. Army Engineer Waterways Experiment Station**
Mobility and Environmental Systems Laboratory
Vicksburg, Mississippi

ARMY-MRC VICKSBURG MISS

APPROVED FOR PUBLIC RELEASE; DISTRIBUTION UNLIMITED

THE CONTENTS OF THIS REPORT ARE NOT TO BE
USED FOR ADVERTISING, PUBLICATION, OR
PROMOTIONAL PURPOSES. CITATION OF TRADE
NAMES DOES NOT CONSTITUTE AN OFFICIAL EN-
DORSEMENT OR APPROVAL OF THE USE OF SUCH
COMMERCIAL PRODUCTS.

PRECEDING PAGE BLANK NOT FILMED

FOREWORD

The study reported herein was conducted by personnel of the Mobility Research and Methodology Branch (MRMB), Mobility Systems Division (MSD), Mobility and Environmental Systems Laboratory (MESL), U. S. Army Engineer Waterways Experiment Station (WES). It was sponsored by the Advanced Development Office, Advanced Manned Missions, Headquarters, National Aeronautics and Space Administration (NASA), Washington, D. C., and was under the technical cognizance of Dr. N. C. Costes of the Space Sciences Laboratory, George C. Marshall Space Flight Center (MSFC), Huntsville, Alabama. The work was performed under NASA Defense Purchase Request No. H-92166A, dated 30 March 1972.

The tests were conducted under the general supervision of Messrs. W. G. Shockley, Chief of the MESL, A. A. Rula, Chief of the MSD, and S. J. Knight and C. J. Nuttall, Jr., former and present Chiefs of the MRMB, respectively, and under the direct supervision of Dr. K.-J. Melzer and MAJ G. D. Swanson of the MRMB, who also prepared this report.

The Elastic Loop Mobility System used in this study was built by the Lockheed Missiles and Space Company (LMSC), Huntsville, Alabama, under NASA Contract NASB-27737 for MSFC and with its cooperation.

Acknowledgment is made to Messrs. C. J. Nuttall, Jr., J. L. Smith, and A. B. Thompson of the MRMB for their advice and support and to Drs. N. C. Costes, MSFC, and W. Trautwein, LMSC, for their general assistance during the conduct of this study.

BG E. D. Peixotto, CE, and COL G. H. Hilt, CE, were Directors of the WES during the conduct of the study and the preparation and publication of this report. Mr. F. R. Brown was Technical Director.

PRECEDING PAGE BLANK NOT FILMED

CONTENTS

	<u>Page</u>
FOREWORD	v
NOTATION	ix
CONVERSION FACTORS, METRIC TO BRITISH UNITS OF MEASUREMENT	xi
SUMMARY.	xiii
PART I: INTRODUCTION.	1
Background	1
Purpose.	2
Scope.	2
PART II: SOIL AND TEST EQUIPMENT.	4
Soil	4
Test Equipment	6
PART III: TEST PROCEDURES AND DATA PRESENTATION	23
Test Procedures.	23
Data Presentation.	31
PART IV: ANALYSIS OF TEST RESULTS	42
Soft-Soil Performance.	42
Obstacle-Surmounting and Crevasse-Crossing Capabilities.	59
Evaluation of Internal Losses.	62
Evaluation of Contact Pressure Distribution.	64
Comparison of ELMS II with Other Running Gears	67
PART V: CONCLUSIONS AND RECOMMENDATIONS	70
Conclusions.	70
Recommendations.	71
LITERATURE CITED	72
APPENDIX A: DATA TABLES	A1

PRECEDING PAGE BLANK NOT FILMED

NOTATION

a	Distance between geometric center point of ELMS II and the point of trailer connection = 0.35 m
b	Distance between geometric center point of ELMS II and trailer axle = 1.42 m
c_{tr}	Cohesion derived from trenching tests, kPa
F_f, F_r	Front and rear shock absorber forces, respectively, N
F_u, F_l	Upper and lower pitch forces, respectively, N
G	Cone penetration resistance gradient, MPa/m
L	Load component transferred through rigid connection to trailer = $M'_p / (b - a)$, N
M, M_a, M_c, M_m	Actual torque, applied torque, torque derived by motor-current method, and torque measured by strain-gage method, respectively, m-N
M_p	Pitch moment at restrained-pitch connection linking ELMS II to dynamometer carriage during phase I tests, m-N
M'_p	Pitch moment at rigid connection linking ELMS II with trailer, m-N
p_c	Contact pressure, kPa
P	Pull, N
P_a	Pull applied to ELMS II-trailer system, N
P_{TR}	Component of trailer weight acting parallel to slope in downward direction = $W_{TR} \sin \alpha$
P_α	Component of ELMS II weight acting parallel to slope in downward direction = $W \sin \alpha$
PC	Pull coefficient = P/W_N , dimensionless
PC'	Pull coefficient corrected for load transfer = P/W' , dimensionless

PRECEDING PAGE BLANK NOT FILMED

PC_T	Towed force coefficient, dimensionless
PN	Power number = $M_\omega/W_N v_a$, dimensionless
PN'	Power number corrected for load transfer = $M_\omega/W'v_a$, dimensionless
PN_{SP}, PN_{20}	Power numbers for self-propelled and 20 percent slip conditions, respectively, dimensionless
r_e	Effective radius of ELMS II loop at the drive drum, m
s	Slip, %
SP	Self-propelled point ($P/W = 0$)
TC	Torque coefficient = $M/W_N r_e$, dimensionless
TC'	Torque coefficient corrected for load transfer = $M/W' r_e$, dimensionless
TP	Towed point ($M = 0$)
v_a	Translational speed of the carriage, m/sec
v_o	Translational speed of carriage at zero slip, m/sec
v_t	Translational speed of ELMS II loop, m/sec
v_{SP}, v_{TP}	Translational speed of carriage at self-propelled and towed points, respectively, m/sec
w	Moisture content, %
W	Load, N
$W_N = W \cos \alpha$	Component of ELMS II weight acting normal to slope, N
W'	Load component acting normal to slope surface, corrected for load transfer = $(W_N - L)$, N
z	Sinkage, cm
α	Angle of slope, deg
α'	Equivalent slope angle, deg
β	Pitch angle, deg
γ_d	Dry density, g/cm^3
δ_f, δ_r	Front and rear shock absorber displacements, respectively, m
η	Efficiency = Pv_a/M , dimensionless
σ_n	Normal stress, kPa
σ_{pl}	Angle of internal friction determined from in situ plate tests, deg
σ_s	Secant friction angle determined from triaxial tests, deg
ω	Angular velocity of the ELMS II, rpm

CONVERSION FACTORS, METRIC TO BRITISH UNITS OF MEASUREMENT

Metric units of measurement used in this report can be converted to British units as follows:

<u>Multiply</u>	<u>By</u>	<u>To Obtain</u>
centimeters	0.3937	inches
meters	3.2808	feet
newtons	0.2248	pounds (force)
meter-newtons	0.7375	foot-pounds
kilopascals	0.1450	pounds (force) per square inch
megapascals per meter	3.684	pounds (force) per cubic inch
grams per cubic centimeter	62.43	pounds (mass) per cubic foot

SUMMARY

Tests were conducted to evaluate the mobility performance of a second-generation Elastic Loop Mobility System (ELMS II) developed by Lockheed Missiles and Space Company for the National Aeronautics and Space Administration (NASA). Performance on level test lanes and slopes of lunar soil simulant (LSS) and obstacle-surmounting and crevasse-crossing capabilities were investigated. In addition, internal losses and contact pressure distributions were evaluated.

To evaluate the soft-soil performance, two basic soil conditions were tested: loose (LSS₁) and dense (LSS₅). These conditions embrace the spectrum of soil strengths tested during recent studies for NASA related to the mobility performance of the LRV. Data indicated that for the tested range of the various performance parameters, performance was independent of unit load (contact pressure) and ELMS II drum angular velocity, but was influenced by soil strength and ELMS pitch mode. Power requirements were smaller at a given system output for dense soil than for loose soil. The total system output in terms of pull developed or slope-climbing capability was larger for the ELMS II operating in restrained-pitch mode than in free-pitch mode.

The angle of the maximum slope that the ELMS II climbed in free-pitch mode on dense soil was 35 deg; on the same soil, but with the system operating in restrained-pitch mode, the angle of the maximum climbable slope was 34 deg, and on loose soil, it was 27 deg. The smaller maximum slope angles for restrained-pitch mode resulted from load being transferred from the ELMS II to the trailer, which was used during the slope tests to stabilize the single unit. If this load transfer can be overcome, for example by replacing the trailer with a second powered unit, this two-unit ELMS should be able to climb slopes with angles up to 38 deg on dense soil and up to about 35 deg on loose soil. The slope-climbing capability can be estimated from results of tests conducted on level ground.

The maximum rigid-step obstacle surmounted was 46 cm high, and the maximum crevasse crossed was 100 cm wide. It can be assumed from the ELMS performance during these tests that obstacles and crevasses with larger dimensions could be negotiated if the trailer were replaced by a second powered ELMS II unit with a pitch-control system in the linkage between the units.

PRECEDING PAGE BLANK NOT FILMED

Internal losses were smaller than those of the first-generation ELMS for torques up to about 60 percent of the total available torque; for higher torques, the reverse was the case. The contact pressure distribution along the longitudinal axis of the loop showed maximum contact pressure occurring toward the middle of the loop, whereas the transverse cross-sectional distribution showed pressure concentrations at the loop edges.

The ELMS II showed an overall superior performance as compared with that of the first-generation ELMS and the wheels used on the U. S. Lunar Roving Vehicles.

PERFORMANCE EVALUATION OF A SECOND-GENERATION
ELASTIC LOOP MOBILITY SYSTEM

PART I: INTRODUCTION

Background

1. Surface mobility of advanced-design roving vehicles will be the key to future lunar and planetary missions extended over large areas. However, the history of the development of all-terrain systems has been marked by a controversy between proponents of wheeled vehicles and those of tracked vehicles. Generally, tracked vehicles have better soft-soil performance and low-speed mobility but more weight and mechanical complexity, resulting in less reliability; whereas wheeled vehicles have better high-speed mobility, less weight, and more efficient drive systems. Wheeled rovers provided sufficient mobility for the early phase of lunar exploration, as demonstrated by the U. S. Lunar Roving Vehicles (LRV) during the Apollo Program and by the Russian Lunokhod I. In 1970, in anticipation of future manned or unmanned extraterrestrial missions, Lockheed Missiles and Space Company (LMSC) developed a running gear that combines the major advantages of wheeled and tracked vehicles: the Elastic Loop Mobility System (ELMS). The first-generation system (ELMS I) was tested at the U. S. Army Engineer Waterways Experiment Station (WES) under the sponsorship of the Advanced Development Office, Advanced Missions Program, National Aeronautics and Space Administration (NASA) through the Space Sciences Laboratory of the Marshall Space Flight Center (MSFC), Huntsville, Alabama. The results of that program showed promising trends in the performance of the system in terms of soft-soil, obstacle-surmounting, and slope-climbing capabilities (Melzer and Green, 1971; Melzer and Trautwein, 1972).

2. Subsequently, LMSC, under NASA contract and technical guidance of the MSFC Space Sciences Laboratory, developed a second-generation system (ELMS II). In early 1972 the WES conducted a short acceptance test program for MSFC, the purpose of which was to determine whether the

system and its components were functioning as required. The acceptance tests were designed so that their results could be used, at least within certain limits, in the extensive mobility performance evaluation to follow.* This mobility performance and evaluation and its results are described herein. Henceforth, the term ELMS will refer to the second-generation Elastic Loop Mobility System (ELMS II), unless otherwise designated.

Purpose

3. The purpose of this study was to conduct a laboratory evaluation of the performance of the ELMS in terms of its soft-soil, slope-climbing, obstacle-surmounting, and crevasse-crossing capabilities.

Scope

4. The program was conducted in three phases. During phase I the ELMS was mounted in a single-unit dynamometer system; and 27 multipass, constant-slip (see paragraph 36) tests were conducted on level surfaces of lunar soil simulant (LSS) prepared to loose (LSS₁***) or dense (LSS₅) consistency. Loads were 565 and 690 N.† The ELMS was either allowed to pitch freely or was restricted to pitch angles (β) of -3, 0, or +4 deg. Angular velocities of the ELMS drums were about 33 and 130 rpm, with corresponding translational drum speeds of about 0.5 and 2.0 m/sec.

5. During phase II the system was tested by a controlled-pull technique (see paragraph 40) on 10 LSS slopes ranging from 0 to 35 deg; the LSS was prepared to dense consistency only. Tests of from two to

* The results of the acceptance tests were submitted as a letter report to NASA-MSFC on 19 July 1972.

** Subscripts to "LSS" denote certain strength characteristics of the simulant and are used in all studies conducted on LSS for NASA.

† A table of factors for converting metric units of measurement to British units is given on page xi.

eight passes each were conducted on each slope. The nominal load was 690 N. Pitch conditions were: free, fully restrained ($\beta = 0$ deg), and elastically restrained (see paragraph 29). The speed range was about the same as that in phase I.

6. During phase III one-step, single obstacles up to 46 cm high and crevasses up to 100 cm wide were used. Tests were run with a load of 690 N. In addition, the internal losses of the ELMS and its contact pressure distribution were evaluated.

7. Where tests were conducted in phases I and II that were similar to the acceptance tests, the results of the acceptance tests were incorporated in the analysis.

PART II: SOIL AND TEST EQUIPMENT

Soil

Description

8. The LSS used in this study was a crushed basalt that had been processed to produce a grain-size distribution approximating that of soil samples collected during the Apollo program (Costes, Farmer, and George, 1972). Generally, the grain-size distribution covered the silt and fine sand ranges. The LSS had the characteristics of a basically cohesionless soil, which, however, exhibited a small amount of cohesion when moist and/or compacted. The mechanical properties of the material have been described in detail elsewhere (Melzer and Green, 1971; Melzer, 1971). This material was used for the program reported herein to allow a direct comparison among the performances of the ELMS II, the ELMS I, and the L.V wheels, which were also tested on LSS.

Preparation

9. Two soil conditions were required for the soft-soil tests: one in which the soil was air-dry and placed loosely, thereby yielding high compressibility and low strength characteristics (LSS_1); and the other in which the soil was moist and compacted, thus yielding a relatively high strength (LSS_5). The average cone penetration resistance gradient (G) of the LSS_1 was 0.30 MPa/m, ranging between 0.09 and 0.84 MPa/m; the G values of the LSS_5 ranged from 3.99 to 9.47 MPa/m, with an average of 6.59 MPa/m. (See table A1.*)

10. The air-dry LSS_1 was processed in place before each test by plowing with a seed fork to a depth of 30 cm and screeding the surface level. The average moisture content of the processed material was 1.0 percent. To prepare LSS_5 , the material was mixed in the soil bin (length = 8.5 m, width = 1.6 m) with an amount of water that would result in a mixture with an average moisture content of about 1.8 percent. The amount of moisture was held constant by covering the test section when

*Tables numbered with the prefix "A" comprise Appendix A.

not in use and occasionally spraying the surface slightly with water to compensate for evaporation. The material was processed before each test by plowing, as was done for LSS₁; but in addition, the soil was compacted with a surface vibrator until the desired density was reached. Finally, the surface was screeded level. The uniformity of each test section was checked by measurements with the WES mechanical cone penetrometer.

11. During phases I and II, each test consisted of one or several passes of the ELMS over the soil, and for each pass the slip condition of the system was changed. The soil was not reprocessed between passes; only the disturbed soil on top was removed and the surface screeded level. This procedure, chosen to lessen the cost of soil processing, seemed justified since the soil underwent only minor changes during the first three to five passes (especially the LSS₅) as long as the slip rates were kept within moderate limits. Furthermore, based on previous experience, these minor changes in soil strength were not anticipated to affect the ELMS performance appreciably within the range of light loads used in these tests.

Soil tests

12. Tests were conducted to determine values of cone penetration resistance, moisture content, and density. Before-traffic values are summarized in table A1; detailed data for each test are given in table A2.

13. Cone penetration resistance. The WES mechanical cone penetrometer was used during the soft-soil performance tests to measure the penetration resistance gradient G . During phases I and II, G was determined prior to the first pass, at five points on the center line of a test section and at five points to the right and five points to the left offset 25 cm from the center line. During phase I, data were also taken along the center line before the second and third passes at five additional points each. These 15 penetrations (5 for each pass) were so close together that no valid data could be taken before the fourth pass (if conducted). During phase II, in addition to the before-traffic penetrations, data were taken at five points along the center line only after the last pass had been conducted.

14. Relative density, dry density, and moisture content. In connection with the soft-soil performance tests, a few density and moisture content measurements were determined gravimetrically by means of a "density box" (Freitag, Green, and Melzer, 1970). In addition, the surface moisture content of each test section was determined for each test. During one of the earlier programs for NASA during which LSS was used, relations among G , dry density, relative density, and moisture content were established (Melzer, 1971, fig. 2). The same relations were used in this study to determine values of dry density and relative density from the measured values of G and moisture content; and density and relative density were monitored primarily by measuring the penetration resistance with the WES cone penetrometer. The minimum, maximum, and average values for LSS_1 and LSS_5 are listed in table A1, together with the volumetrically determined values of density, relative density, and moisture content.

15. Shear strength. Angles of internal friction based on vacuum triaxial and in situ plate shear tests, and cohesion based on trenching tests were determined for various relative densities and moisture contents in earlier studies (Melzer and Green, 1971; Melzer, 1971). From these relations average angles of internal friction and average values of cohesion were determined for the soil conditions tested during this study and are given in table A1.

Test Equipment

ELMS II

16. The ELMS mounted in the dynamometer system during phase I is shown in figs. 1, 2, and 3, and during slope tests of phase II in fig. 4. The unit is 1.66 m long and 36 cm wide, and consists of a power storage space (battery box), two drive drums with brushless d-c drive motors mounted internally (maximum torque output limited to 82 m-N), and a continuous loop fabricated from Beta III titanium alloy (fig. 1). Seventy polyurethane foam-type grousers are mounted to the loop to provide traction and favorable pressure distribution. Nylon knobs affixed to

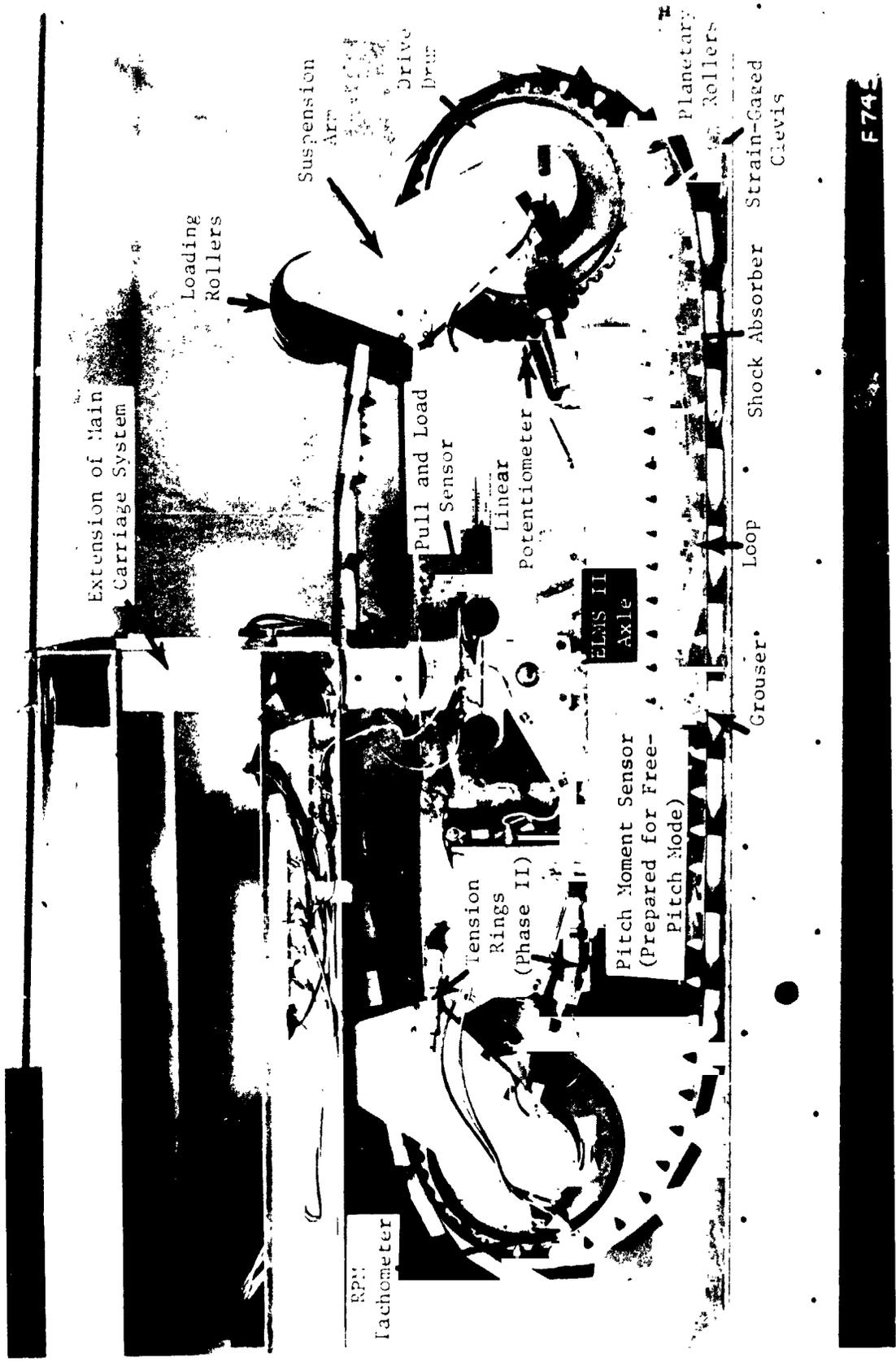


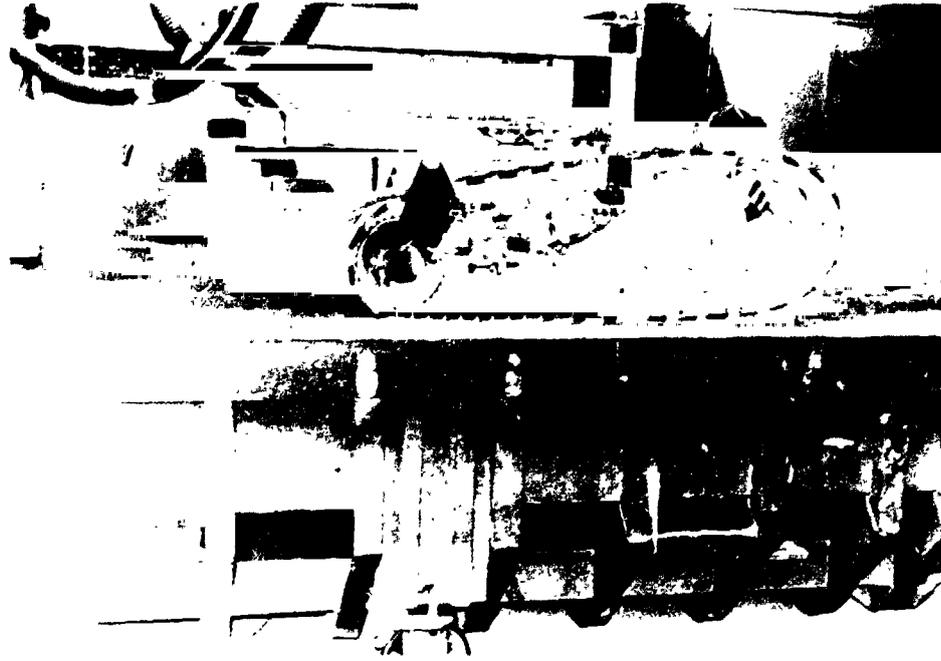
Fig. 1. Close-up of ELMS II in WES dynamometer system

F74

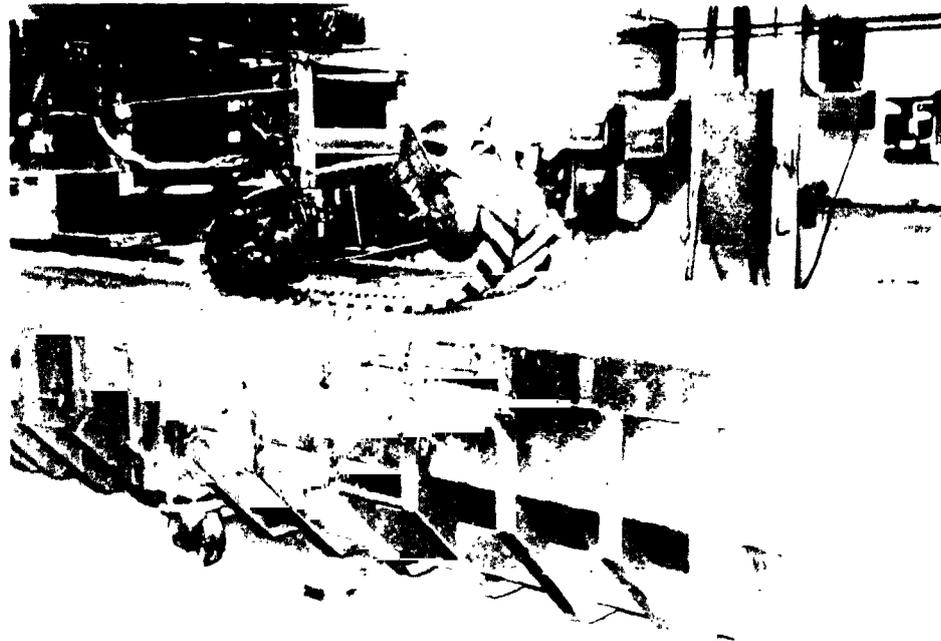


Fig. 2. ELMS II mounted in WES dynamometer system

F745-3

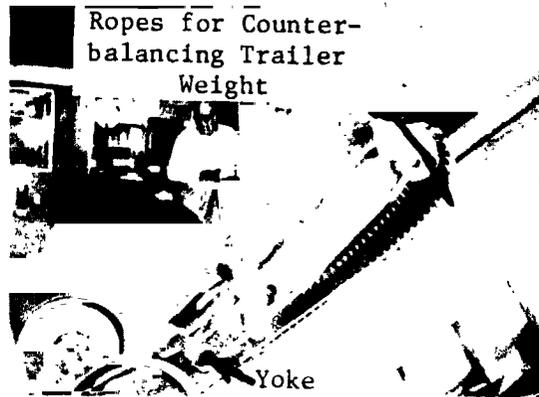


a. Slip = 4.0 percent; pitch angle = +6 deg

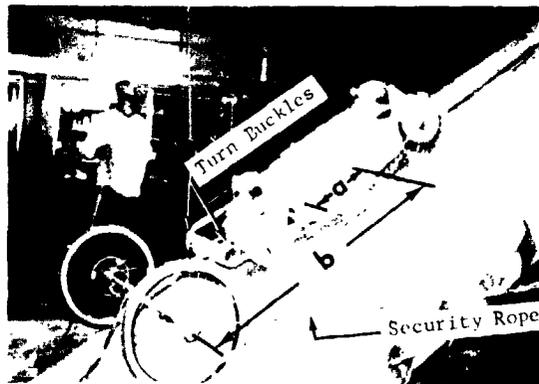


b. Slip = 37.8 percent; pitch angle = +10 deg

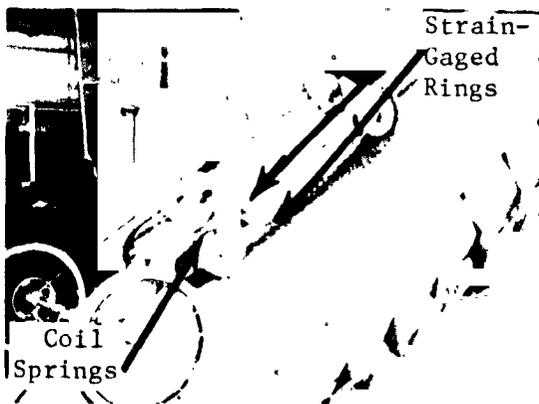
Fig. 3. ELMS II during tests in phase I, free-pitch mode, soil condition LSS₅, load: 565 N, drum speed: 0.5 m/sec



a. 35-deg slope; free-pitch mode



b. 34-deg slope; fully restrained-pitch mode



c. 34-deg slope; elastically restrained-pitch mode

Fig. 4. ELMS II during tests in phase II, soil condition LSS₅, drum speed: 0.5 m/sec

the loop engage planetary rollers with frictionless pivots, which are attached to the drum. This arrangement provides a propulsion system with relatively small internal energy losses. A more detailed description of the ELMS, its components, and instrumentation is given by Trautwein (1972) and Costes and Trautwein (1973). However, a few details on the instrumentation are given in the following paragraphs because of their importance to this test program.

17. Measurements of torque. Two methods for measuring torque were provided by the manufacturer: the "motor-current method" and the "strain-gage method." In the first, calibration curves of motor current versus torque had been established (Trautwein, 1972, figs. 7-6 and 7-7). By monitoring the motor current during each test, the torque could be determined from these calibration curves. However, in about 70 percent of the acceptance tests, the torque measured by this method was found to be too small. For example, if maximum torque was applied by forcing the ELMS to stall, the maximum torque measured was not more than about 65 m-N, instead of 82 m-N one would expect*. Unfortunately, a recalibration of the motor current was impossible during this test program, so torque had to be measured by the strain-gage method.

18. In the strain-gage method, the drive torque tubes that connect the motors with the drive drums were equipped with two strain gages each. The sum of the four sensor outputs yielded the total output delivered by the two motors. The calibration of the sensors was given to WES by LMSC (Trautwein, 1972, table 7-2). However, after the acceptance tests, LMSC informed the WES that the strain-gage readings are influenced by the condition under which the ELMS is tested.** For example, readings taken during level-ground tests with the ELMS mounted in the dynamometer

* These findings were later confirmed during phases I and II of the program reported herein; the torques measured using both methods are listed in tables A3 and A5.

** Positioning of the ELMS in other than horizontal position caused shift of the bending moment on the torque tubes, which influenced the strain-gage readings.

system (phase I) would correspond to a different torque from those taken during slope tests (phase II). Therefore, separate calibrations were made for each test condition. Each calibration consisted of applying two or three known external torques that were counterbalanced with the ELMS drive motors.

19. Calibration curves were obtained as follows: The torque M_m measured by the strain gages was plotted versus the known external torque M . Fig. 5 shows the calibration curve established for the evaluation of the tests conducted during phase I, and fig. 6 shows the family of calibration curves used for the analysis of the phase II and phase III tests. It should be pointed out that in the phase II tests (fig. 6), the calibration curves were established only for the torque range expected for a certain test. As the scatter of the data shows, it was extremely difficult to obtain a good set of calibration data for the phase II tests.

20. Measurement of angular drum velocity. Drum velocity was measured by tachometers (furnished by Lockheed) mounted inside each drum; an additional tachometer (furnished by WES; fig. 1) was mounted on the outside of the front drum to indicate ELMS position in addition to drum rpm, and a relation of rpm versus output voltage was established.

21. Measurement of shock absorber forces and displacements. Shock absorber forces were measured by two strain-gaged clevises, one mounted between the outer end of each shock absorber piston rod and the corresponding suspension arm of the ELMS (fig. 1). Shock absorber displacements were measured by potentiometers connected to the suspension arms (fig. 1). Calibrations for the potentiometers and the strain-gaged clevises were provided by Lockheed (Trautwein, 1972, table 7-3 and fig. 7-8). However, one of the clevises broke during the program and was replaced and recalibrated by the WES.

22. Measurement of sinkage. Sinkage was not monitored continuously. However, it was measured during phase I before and after each pass by means of a point gage at six places on the center line of the rut produced by the ELMS. This method was chosen since sinkage did not appear to be one of the important performance parameters because of the low contact pressures (good flotation characteristics) involved. Thus,

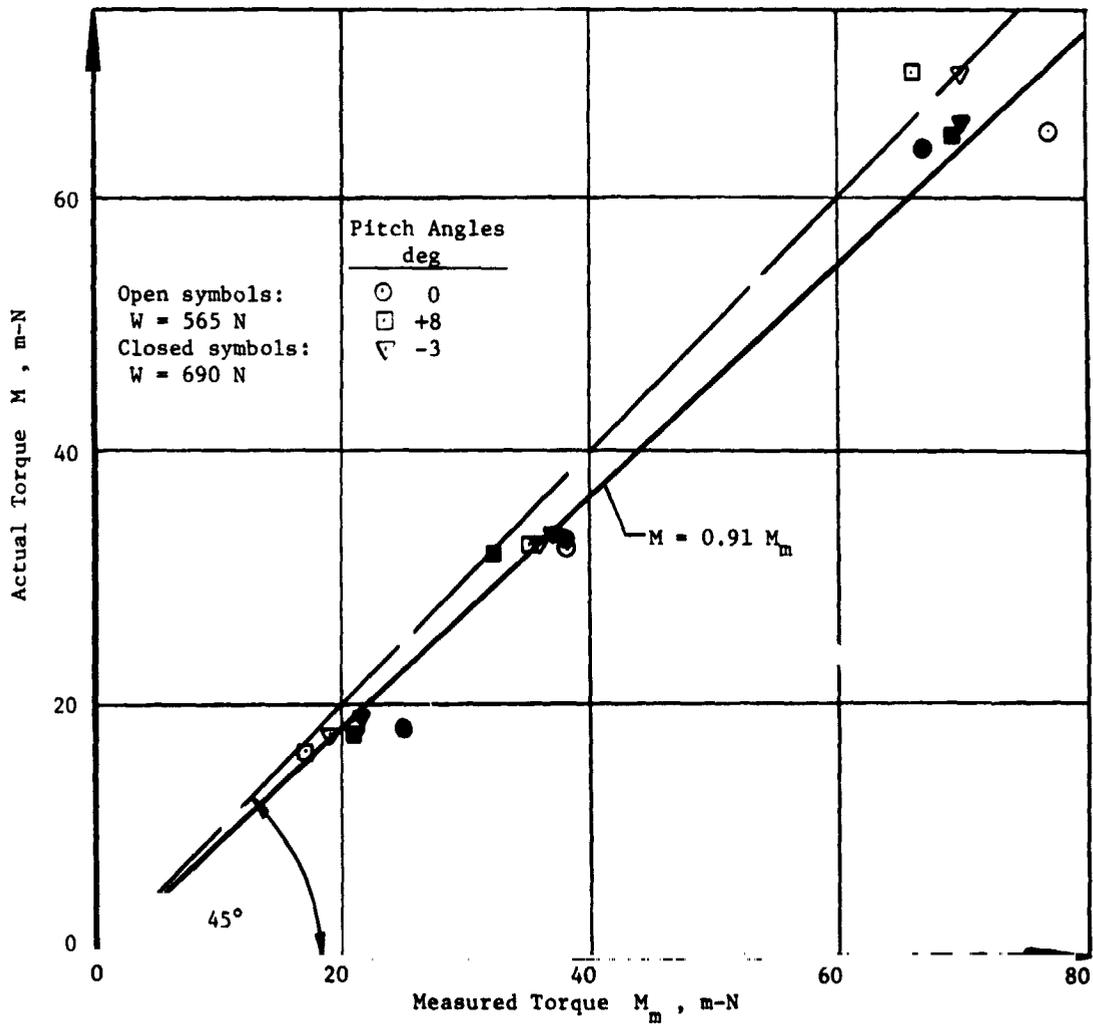


Fig. 5. Calibration for strain-gage torque method for phase I

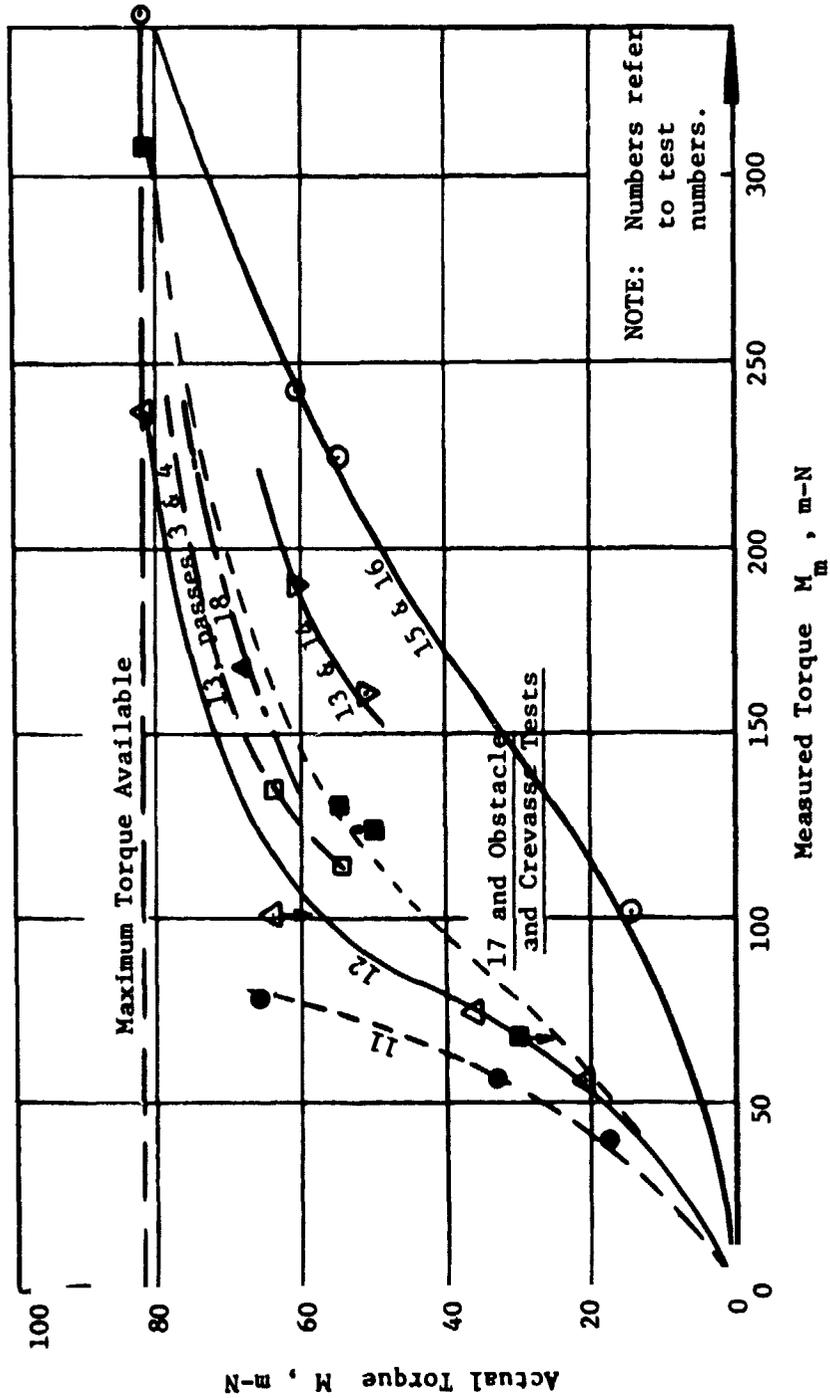


Fig. 6. Calibration for strain-gage torque method for phases II and III

the data channel usually used to record sinkage could be used to monitor one of the other more important parameters.

Dynamometer system

23. The WES dynamometer system (figs. 1 and 2) was modified to accept the ELMS. Four horizontal support beams (two on each side of the system) were mounted to the main carriage so that they could pivot freely as cantilevers. The beams were connected by joints to two vertical ELMS support beams at the front end of the system (one on each side). This "parallelogram" arrangement of the three beams on each side assured that the longitudinal axis of the vertical support beam remained perpendicular at all times, regardless of the angle to the horizontal the two support beams might assume during a test; for example, due to sinkage. This arrangement was necessary because the sensors for measuring vertical load and horizontal pull were mounted to the vertical support arm (fig. 1) and had to be maintained in the same position relative to the horizontal. Any deviation from the horizontal or vertical would have distorted these measurements.

24. Three-component sensors. Two three-component sensors were designed and fabricated by the WES especially for this program, and were mounted on either side of the vertical support frame (figs. 1 and 2). The sensors were machined and strain-gaged so that two forces and one moment could be measured. The two forces were vertical load acting on the ELMS (created by counterbalancing the system; see weight pan in fig. 2) and horizontal pull developed by the ELMS. The sensors were designed to be capable of measuring a maximum force of 670 N in either direction.

25. Original plans called for using the three-component sensors to measure the pitch moment occurring when the ELMS was restrained. However, checkouts during calibration showed that pitch moment measurements were influenced by pull and/or load, and this idea was abandoned.

26. Pitch moment sensors. Because the pitch moments could not be measured as originally planned (paragraph 25), a moment arm was attached to each of the three-component sensors (figs. 1 and 2). The ELMS was mounted to these arms by stub axles, which led to ball bearings inside

the part of the moment arms attached to the sensors. When the ELMS was not restrained, it pivoted freely about this point (figs. 3a and 3b). The pitch angle was measured by a protractor mounted to the left moment arm (not seen in figs. 1 and 2). For the tests in restrained-pitch mode, a load cell of 1350-N capacity was mounted to each of the moment arms and connected to the chassis of the ELMS (fig. 1). These load cells indicated the pitch forces exerted by the ELMS when being restrained, and the corresponding pitch moment could be calculated because the length of each moment arm was known.

27. Damping system. To avoid some of the vertical oscillation of the parallelogram system (paragraph 23), which occurred especially when the ELMS was tested at high speeds on relatively firm soil, a viscous-damping system was designed. It consisted of a frame that was connected at one end by a load cell (2200-N capacity) to the lower horizontal support beams (fig. 2). The other end rotated freely about an axle mounted to the frame of the main carriage. At a distance of about one-third of its length, the frame of the damping system was connected by two rolling diaphragm cylinders to the main carriage. The cylinders contained a low viscous fluid (oil). This arrangement provided the damping of vertical motion of the parallelogram system. A potentiometer and a load cell were available to measure vertical displacement and force, respectively, due to damping, but these measurements were not monitored during this program because of the limited number of channels available in the recording equipment.

28. Main carriage. The main carriage of the dynamometer system was the same as that used in previous NASA programs. It carries sufficient instrumentation cables to provide for up to 30 channels of analog signals. It can operate at speeds up to 8 m/sec, and can be held at constant speed, uniformly decelerated, or uniformly accelerated in a given test run. Speed was measured by a tachometer; also measured were time and distance traveled. Thus, with the actual speed v_a of the carriage and the ELMS drum rpm (see paragraph 20) known, the slip at the loop-soil interface could be determined as follows (this procedure was

developed by the sponsor and used at his request*). From plots of torque M and pull P , measured during tests of phase I, versus actual speed v_a , the speed values v_{TP} (carriage speed at towed point) and v_{SP} (carriage speed at self-propelled point) corresponding respectively to $M = 0$ and $P = 0$ were obtained. The effective radius r_e of the ELMS loop was then calculated from

$$r_e = \frac{v_o}{\omega} \quad (1)$$

where

$$v_o = \frac{v_{TP} + v_{SP}}{2}, \text{ assumed to be the carriage speed at zero slip,}$$

$$\omega = \frac{2\pi \text{ rpm}}{60}.$$

Using this r_e , slip(s) expressed as a percentage is:

$$s = \frac{v_t - v_a}{v_t} 100 \quad (2)$$

where $v_t = \omega r_e$. This method allows direct determination of r_e developed under a particular testing condition and assures in the subsequent slip calculations (equation 2) that the "towed point" always occurs at zero or negative slip values, whereas the "self-propelled point" always occurs at zero or positive slip values. The values for r_e evaluated from the test results of phase I are listed in table A3. To evaluate slip in phase II, r_e values were chosen from test conditions (speed, load, soil density) of phase I that were comparable to the phase II conditions under consideration (table A5). The r_e values evaluated varied between 0.148 and 0.155 m. This is close to 0.159 m that one obtains from

$$r_e = \frac{p \cdot n}{2\pi} \quad (3)$$

where

p = straight-line distance between teeth on track = 0.05 m.

n = number of teeth in contact on the drive drum = 20.

*Personal communication with Dr. Costes, MSFC.

Trailer

29. For the slope tests (phase II) and obstacle-surmounting and crevasse-crossing tests (phase III), a two-wheeled trailer that had been fabricated by LMSC was attached to the ELMS (fig. 4). The ELMS chassis was connected to the trailer yoke by four stiff arms (fig. 4a). The yoke consisted of two outer transverse tubes (to which the four trailer arms were connected) that rotated around one common inner tube (which was connected to the trailer axle by one arm). Thus, this configuration allowed the ELMS to rotate freely about the trailer yoke (fig. 4a). This rotation could be prevented by locking the two outer tubes to the inner tube; this created the fully restrained pitch mode (fig. 4b). The rigidity of this restraint was decreased by replacing rigid turnbuckles of the upper arms (fig. 4b) with coil springs (fig. 4c), resulting in the so-called "elastically restrained" pitch mode.

30. At the connecting points of the four trailer arms and the ELMS chassis, four strain-gaged rings (tension rings in fig. 1) provided for measurements of the axial forces occurring in the trailer arms (fig. 4c). Calibration data were provided by LMSC (Trautwein, 1972, table 7-1). With these measurements the pitch moments occurring during tests conducted in restrained-pitch modes were calculated (Trautwein, 1972, p 7-2):

$$M_p = \frac{1}{2} h(F_u - F_l) \quad (4)$$

where

M_p = pitch moment, m-N; counterclockwise = negative.

h = vertical distance between upper and lower trailer arms = 0.186 m.

F_u = sum of forces occurring in the two upper arms;
tension = positive, compression = negative.

F_l = sum of forces occurring in the two lower arms;
tension = positive, compression = negative.

Recording systems

31. Phase I. The primary data recording system was an on-line digital computer, which was used in previous NASA studies (Green and Melzer, 1971; Melzer and Green, 1971). With this system, electrical (analog) signals reach the computer through cables in a raw form without signal conditioning. The signals are converted to digital form by the computer and stored on magnetic tape for subsequent data processing. Alternatively, the analog signals can be recorded on tape and digitized later. This alternative method was used during this program. Because of the multitude of variables to be recorded, two tape recorders had to be used. The estimated error of the system is about 4 percent. Only results from this primary recording system were used to analyze phase I results.

32. A secondary recording system was a 36-channel, direct-writing oscillograph, which requires signal conditioning. This system allows the test engineer to take a quick look at some of the more important data as tests progress. The accuracy of the oscillograph readings depends on the scale used and the expertise of the reader. The results obtained are estimated to be accurate to within 6-8 percent.

33. Table 1 lists the parameters transmitted by cables to the recording system, as well as the average parameters as they were finally output by the computer and used for the analysis (tables A3 and A4).

Table 1

<u>Recording System</u>		<u>Measured Parameter</u>	<u>Final Output</u>
<u>Magnetic Tape</u>	<u>Oscillograph</u>		
x	x	Left load	} W
x	x	Right load	
x	-	Left raw pull*	-
x	-	Right raw pull*	-
x	x	Acceleration	-

(Continued)

*Not corrected for inertia effects.

Table 1 (Concluded)

Recording System		Measured Parameter	Final Output
Magnetic Tape	Oscillograph		
x	x	Left pull**	P
x	x	Right pull**	
x	-	Strain Gages { Left front torque Right front torque Left rear torque Right rear torque	-
x	-		-
x	-		-
x	-		-
x	x	Sum of front torques	M
x	x	Sum of rear torques	
x	x	Front motor-current torque	M _c
x	x	Rear motor-current torque	
x	-	Left pitch moment	M _p
x	-	Right pitch moment	
x	-	Shock Absorbers { Front force† Front displacement† Rear force Rear displacement	F _f
x	-		δ _f
x	-		F _r
x	-		δ _r
x	x	ELMS II drum rpm	rpm; v _t
x	x	Carriage speed	v _a
-	x	ELMS position	-
-	x	Carriage position	-
x	x	Digital Data Acquisition System (DDAS) pulse	-
-	-	Sinkage; manually by point gage	z

**Corrected for inertia effects (see paragraph 38).

†Not measured during restrained-pitch tests.

34. Phase II. The primary recording system was a magnetic tape recorder, as in phase I; however, at the time at which these tests were conducted, only one tape recorder (instead of two as in phase I) was available. Therefore, some of the parameters were recorded only on the oscillograph (pull; forces and displacements occurring at the shock absorbers). Portions of data were transmitted to the recording station directly by cables and portions by a telemetry system furnished by the WES

(Lessem, 1972). Table 2 lists the parameters recorded, the transmission and recording systems used, and the average parameters as they were finally output by the computer and used for the analysis (table A4).

Table 2

Recording System		Transmission System*	Measured Parameter	Final Output
Magnetic Tape	Oscillograph			
-	x	1	Pull	P
x	x	1	Strain Gages { Left front torque Right front torque Left rear torque Right rear torque	M
x	x	1		
x	x	1		
x	x	1		
x	x	2	Front motor-current torque	M _c
x	x	2	Rear motor-current torque	
x	x	1	Left upper pitch force	F _u } M _p
x	x	1	Right upper pitch force	
x	x	1	Left lower pitch force	F _l }
x	x	1	Right lower pitch force	
-	x	2	Shock Absorbers { Front force Front displacement Rear force Rear displacement	F _f
-	x	2		δ _r
-	x	2		F _r
-	x	2		δ _r
x	x	2	ELMS II drum rpm	rpm; v _t
x	x	1	ELMS II-trailer speed	v _a
-	x	1	ELMS II position	-
x	x	1	DDAS pulse	-
-	x	2	Battery voltage	-

* 1 = signals transmitted by cables; 2 = signals transmitted by telemetry system.

35. Phase III. For the obstacle-negotiating and crevasse-crossing tests, the recording equipment of phase II was used. During the tests to evaluate the internal losses of the ELMS and its contact pressure distribution, the same equipment was used as was used in phase I; however, five data channels were disconnected to make them available for connection

to the five pressure cells mounted in the specially fabricated grouser to measure the contact pressure (paragraph 49).

PART III: TEST PROCEDURES AND DATA PRESENTATION

Test Procedures

Phase I: Soft-soil performance tests with single unit on level ground

36. Constant-slip test technique. During phase I of the program, a constant-slip test technique was used: the drum rpm and carriage speed of the ELMS were programmed to achieve a desired slip (see paragraph 28) and were held constant during a specific pass. Generally, under a given test condition, data on the mobility performance of the ELMS were obtained at about five* different slips to cover the range of most interest (from about -5 percent to +30 percent). Actual slips obtained ranged from -10.2 to +37.8 percent. Two drum velocity levels were tested, about 33 and 130 rpm. The corresponding translational speeds of the loop were about 0.5 and 2.0 m/sec. However, because the torque output of the motors was limited to 82 m-N (paragraph 16), at higher slips the actual drum rpm had a tendency to deviate from the design rpm whenever there was no available torque to maintain the latter. This change was more drastic at higher rpm levels than at lower. The full range for the lower level was 26.9 to 41.9 rpm, and for the higher level, 51.2 to 132.2 rpm. The rpm ranges, together with the slip range, resulted in actual carriage speeds from 0.31 to 2.13 m/sec.

37. During these tests, the ELMS was subjected to two loads, 565 N and 690 N, covering the range of loads acting perpendicular to the slopes on which the system was tested during phase II. The system was tested in two pitch modes, free and restrained. In the latter mode, the ELMS was restrained to three different pitch angles (β): -3 deg (nose-down position), 0 deg, and +4 deg (nose-up position). Test soils were LSS₁ and LSS₅. Test conditions and average parameters measured are presented in table A3.

* This number varied between 2 and 6 depending on the velocity at which the system was tested. For example, drum rpm = 30 was considered the basic velocity; thus, more slips were tested for this level than for drum rpm = 130, the second velocity condition.

38. Programmed-slip test technique. The test results from phase I were supplemented by results from four selected tests conducted during the acceptance test program (paragraph 2). During the latter program, a programmed-slip test technique was used.* The tests were started in the negative slip range,** i.e. the translational speed (v_a) of the carriage was greater than the speed (v_t) of the ELMS drums. The carriage was slowed at a programmed, uniform rate ($v_t = \text{constant}$) to cause the system to pass through the towed condition (torque $M = 0$), the zero percent slip condition ($v_a = v_t$), the self-propelled condition (pull $P = 0$), etc., as slip was progressively increased up to about +70 percent. The measured raw pull was corrected for inertia effects caused by the deceleration of the carriage system. Three tests were conducted at drum rpm of about 31, and one at 110. The test load was 565 N, and the pitch modes were free and restrained at $\beta = 0$ deg. The soil properties were close to that of soil condition LSS₁. Test conditions and some pertinent performance parameters are presented in table A4.

Phase II: Soft-soil performance tests with ELMS II-trailer configuration on slopes

39. Slopes were constructed by preparing the soil to the desired density in one of the soil bins used during phase I (see paragraph 10) and positioning the bin in one of the large stationary soil pits of the WES test facilities (fig. 7). After the soil data had been collected (paragraphs 12-14), the soil bin was lifted at one end by a crane until the desired slope was reached (figs. 4 and 7). The ELMS II was guided by a remote-control system (Lessem, 1972) that allowed an operator to start and stop the unit as desired.

40. Controlled-pull tests. Each test series on a given slope consisted of up to eight passes. The number of passes depended on the magnitude of the slope angle (smaller with increasing slope angle) and

* Previous testing with wheels (e.g. Melzer, 1971) has shown that, generally, the various test techniques (constant-slip, programmed-slip, etc.) do not influence the mobility performance parameters for a given test condition.

** Except for tests Nos. A-72-002-6 and -006-6, which were started in the positive slip range.

Rope Leading Over Pulley
Arrangement to Rear End
of Trailer

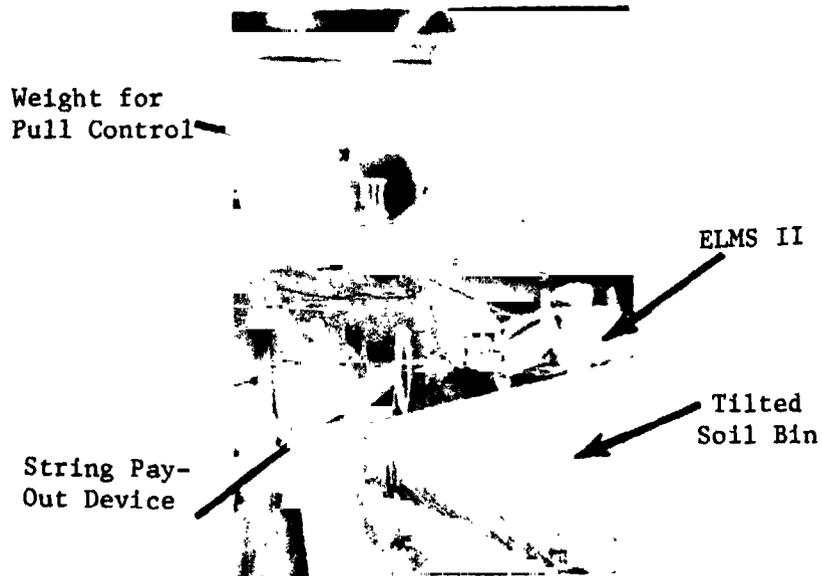


Fig. 7. Test setup for phase II, slope tests

on how much the soil surface was disturbed during traffic. During the first pass, no pull was applied to the ELMS-trailer configuration. After the first pass, pull was held constant during each specific pass in the following manner. A load cell was attached to the rear end of the trailer for recording pull. This load cell was connected with a rope, which led over a friction-free pulley arrangement to a deadweight hanging from the ceiling of the building (fig. 7). During the test run the weight provided a constant pull, which was monitored by means of the load cell. The pull was increased in small increments from pass to pass until the maximum pull the system was able to develop on a given slope was reached. When the system attempted to climb the maximum possible slope, the trailer-weight component acting parallel to the slope surface was counterbalanced (fig. 4a). As a consequence, the slip developed freely for a given condition, and measurements indicate that it was essentially constant during a specific pass.

41. Drum speeds were normally set constant for a given test. The majority of the tests were conducted at an average drum rpm of about 33. Only a few spot-check tests were conducted at higher rpm. Because of the torque limitations of the system (paragraph 16), the two following rpm ranges were actually tested: (a) from 27.3 to 35.6 rpm, and (b) from 92.6 to 123.8 rpm. These ranges, together with the overall range of slip conditions (0.6 to 70.3 percent), resulted in actual speeds of the ELMS-trailer system from 0.14 to 1.90 m/sec.

42. The actual speed was measured by a string pay-out device: A string, attached to the rear of the trailer, was connected to a pay-out device with a friction-free pulley. As the ELMS proceeded forward, the string was "paid out," which caused the pulley to turn. The rpm of the pulley was measured by a tachometer and indicated the actual speed of the ELMS-trailer system.

43. The weight of the ELMS was 690 N and that of the trailer 120 N. Three pitch modes were used (paragraph 29): free, fully restrained, and elastically restrained. The tests were conducted on LSS₅. The slopes ranged from 0 to 35 deg. Test conditions and average parameters measured are presented in table A5.

44. Programmed-pull tests. During the acceptance test program, three tests were conducted on LSS slopes. Results from only one (A-72-009-6), which was conducted on a 27-deg slope, could be used (pertinent data are listed in table A6) to supplement the data from the tests described above, since this was the only test in which torque was measured by the strain-gage method (paragraphs 17-19). This test was conducted as a programmed-pull test, i.e. the pull was increased during the test by means of the string pay-out device (see paragraph 42) until the ELMS-trailer configuration stalled. With this test technique, the system passed very rapidly through the lower slip range at the start of the test; and as a consequence, reliable data for the lower slip range were difficult to collect. For this reason, only the controlled-pull test technique (paragraph 40) was used in the main program.

Phase III: Miscellaneous tests

45. Obstacle-surmounting tests. The obstacles consisted of 5-cm-high, 10-cm-wide wooden planks placed on top of each other; the overall heights were varied by simply changing the number of planks used. Fig. 8 shows the ELMS in free-pitch mode negotiating a 46-cm-high obstacle. The trailer was attached to the ELMS for these tests in the same manner as for the slope-climbing tests (paragraph 29), and the system was guided by remote control (paragraph 39). The unit was placed approximately one-half loop length away from an obstacle and allowed to approach it at creep speed. The drum speed could be varied during a specific run if this was desirable. Whenever the ELMS successfully negotiated a given obstacle, the test was continued until about half the length of the ELMS had passed. During such tests, distance and torque were recorded. Pertinent results are presented in table A7.

46. Crevasse-crossing tests. Crevasses were created in the same soil bin (in horizontal position) as that used for the tests in phase I. A 1.2-m-wide, 0.3-m-deep trench was dug into the soil across the test path. The width of the trench (width of the crevasse) was varied according to the crevasse-crossing capabilities of the ELMS. The soil surfaces on either side of the crevasse were covered with plywood to



Fig. 8. ELMS II negotiating 46-cm-high obstacle,
load 690 N

prevent destruction of the edges of the crevasse. As in the obstacle-surmounting tests, the trailer was attached to the ELMS and the system was guided by remote control. Arbitrary speeds of 0.5 to 1.5 m/sec were used in these tests: drum speed could be varied during a specific run. The width of the crevasse was increased until the ELMS could no longer successfully cross. A record of torque and distance was obtained during these tests. Pertinent test results are presented in table A7.

47. Internal losses. A special method was used to investigate whether the ELMS II had smaller internal losses than the ELMS I. The ELMS was first mounted in the dynamometer system (figs. 1 and 2); next, two small, almost frictionless roller-skate wheels were mounted to the service platform; then the ELMS was lowered onto the wheels and subjected to test loads of 565 or 690 N. The torque developed by the motors was measured by the strain-gage method while the ELMS was lifting a weight from the floor by means of a cable attached to the loop. (This method was the same as "method B" used during the tests to evaluate the internal losses of the ELMS I; Melzer and Green, 1971, p 24).

48. ELMS drum rpm was changed from test to test to cover a range from 32 to 97 with no external torque being applied. However, a series also was conducted by applying external torques ranging from 0 to 39 m-N, while the system was being loaded with 565 N or 690 N. This series was conducted with a drum rpm of only 16; because during the relatively short time required for the ELMS to lift the weight from the floor for the purpose of developing the external torque, no reliable data could be collected at higher rpm. The results are discussed in paragraphs 85-87.

49. Contact pressure distribution. To evaluate the contact pressure distribution at the loop-soil interface, a special grouser built by LMSC was mounted to the ELMS loop (fig. 9). The grouser contained five pressure cells arranged along the long axis of the grouser, i.e. at an angle of about 60 deg to the direction of travel, with cell 5 positioned at the outer loop edge and cells 4, 3, 2, and 1 positioned in sequence toward the loop center (see figs. 28b and 29b). Calibration data for the sensors were furnished by LMSC (Trautwein, 1972, table 7-4).



Fig. 9. Close-up of grouser instrumented for measuring contact pressure distribution

During the tests, the ELMS was mounted in the dynamometer system (figs. 1 and 2) and moved over the prepared soil surface at "creep" speed for about the length of one-half revolution of the loop. Pressure data and distance traveled were measured.

50. Four tests were conducted according to the matrix shown in table 3.

Table 3

Load, N	Soil Condition	
	LSS ₁	LSS ₅
565	x	x
690	x	x

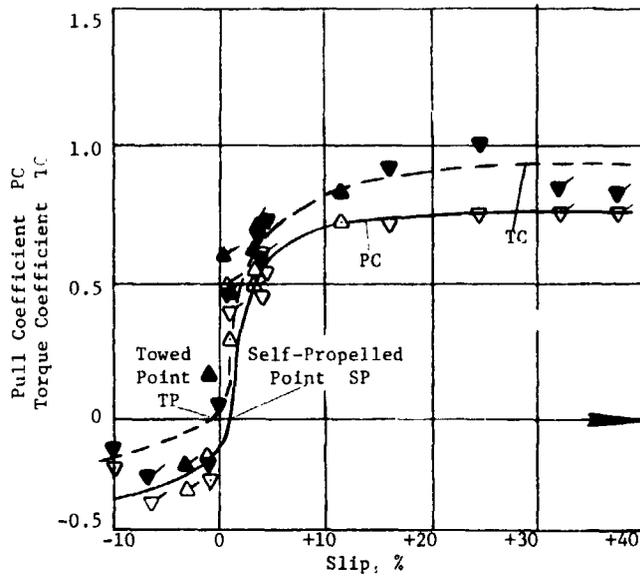
Difficulties in obtaining response from the pressure cells occurred during the tests on LSS₅; sinkage was extremely small, and the pressure cells were not in full contact with the soil. This occurred because the cells were deeply embedded in the grouser and so were not flush with the outer grouser surface. Consequently, the cells gave erroneous readings and sometimes did not respond at all. For this reason, only the results of the tests conducted on LSS₁ are discussed in the analysis (paragraph 88). Even on the softer LSS₁ difficulties were encountered. At a 690-N load, only cells 1, 3, and 5 (PC1, PC3, and PC5 in fig. 28b) functioned; at a 565-N load, only PC1 and PC5 functioned (see fig. 29b).

Data Presentation

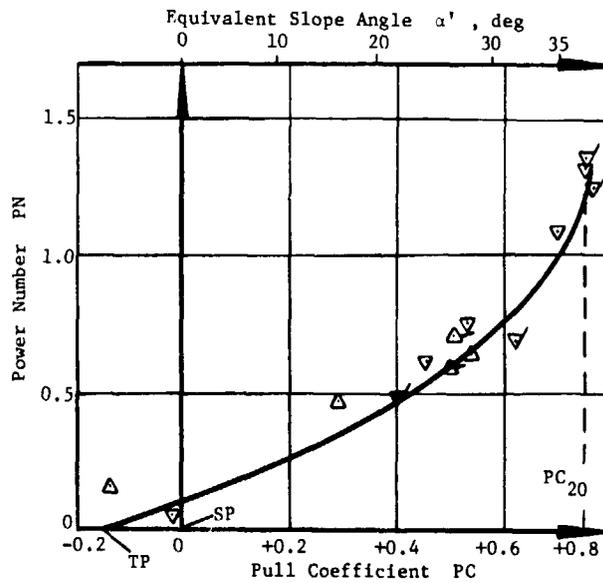
Phases I and II: Soft-soil performance tests on level ground and on slopes

51. Basic performance parameters and relations. Three basic relations were used in presenting the data of the ELMS performance in soft soil (phases I and II): (a) pull coefficient PC (P/W_N) versus slip, (b) torque coefficient TC ($M/W_N r_e$) versus slip, and (c) power number PN ($M\omega/W_N v_a$) versus PC and/or versus equivalent slope angles α' . * Relation (c) was finally chosen as the main basis of analysis because it implicitly contains relations (a) and (b). For example, three major characteristic

*See paragraph 57 for definition of "equivalent slope angle."



a. Pull and torque coefficients as functions of slip (open symbols: PC; closed symbols: TC)



b. Power number as function of pull coefficient and equivalent slope angle

LEGEND		
Load		
rpm	565 N	690 N
33	▽	△
100	▽	△

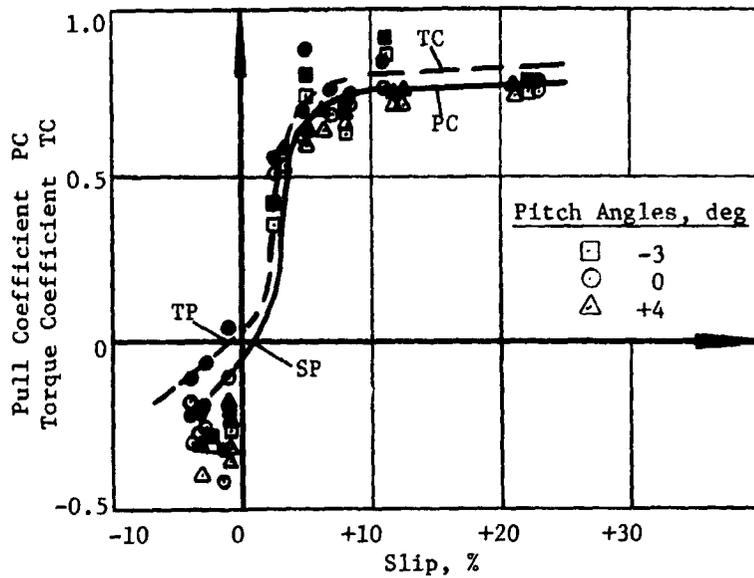
Fig. 10. Performance relations from phase I tests, free-pitch mode, soil condition LSS₅

conditions can be identified in fig. 10a (PC and TC versus slip): the towed condition TP, where torque is zero and the force required to tow the running gear is measured; the self-propelled condition SP, where no pull is developed, i.e. a condition corresponding to one in which the vehicle is traveling on level ground without developing additional pull; and the 20 percent slip condition, where in most instances the maximum pull is developed with no excessive torque being input, and beyond which point the system becomes not only progressively more inefficient but also less effective in developing pull. All three of these conditions can be identified relatively easily also in fig. 10b, where PN is plotted versus PC.*

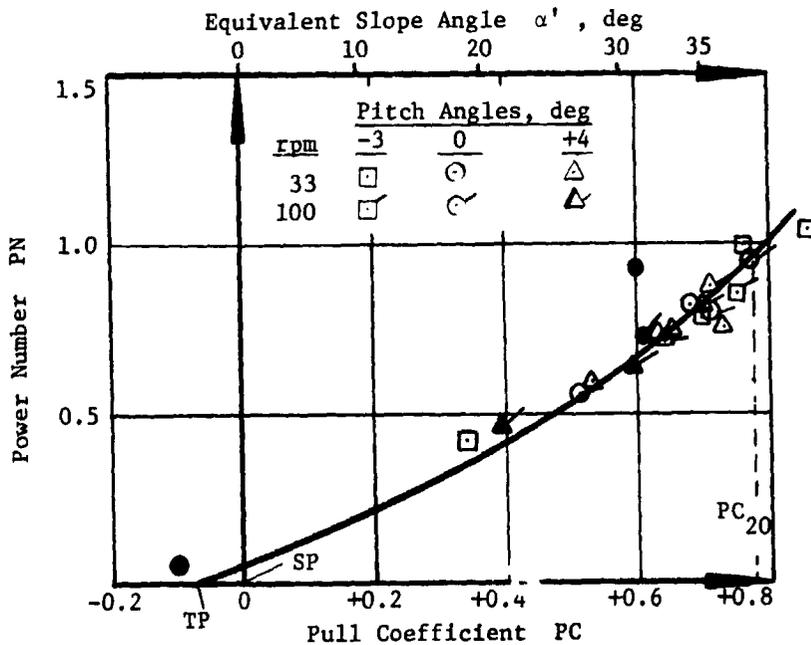
52. The manner in which relations (a), (b), and (c) above were used in conjunction with data obtained through the various test techniques is described in the following paragraphs. In some instances, the relation between efficiency η ($Pv_a/M\omega$) versus PC was used as the basis for comparing various testing conditions. In addition, pitch angles, pitch moments, and energy dissipated in the shock absorbers (product of displacement and force in axial direction; see paragraph 21) were analyzed whenever it seemed appropriate. All performance parameters used are listed in tables A3-A6.

53. Constant-slip and programmed-slip test techniques. Relations of PC versus slip, TC versus slip, and PN versus PC from phase I tests (constant-slip) are displayed in figs. 10a and 10b for tests on LSS₅ and in free-pitch mode. Each data point in a given relation represents an average of about 70 signals obtained from the record of one pass of the ELMS under a given testing condition. The curves plotted represent relations of best visual fit of the data. Figs. 11a and 11b show the results of the tests conducted on LSS₅ under restrained-pitch mode.

* It must be pointed out, however, that no negative power requirements were plotted in the PN-PC diagrams (e.g. fig. 10b) in the framework of this study. Thus, the location of the towed point TP in these diagrams was not only determined by the general trend of a specific PN-PC relation, but also by the trend that corresponding PC and TC versus slip relations showed in the negative slip range (e.g. fig. 10a).



a. Pull and torque coefficients as functions of slip (open symbols: PC; closed symbols: TC)



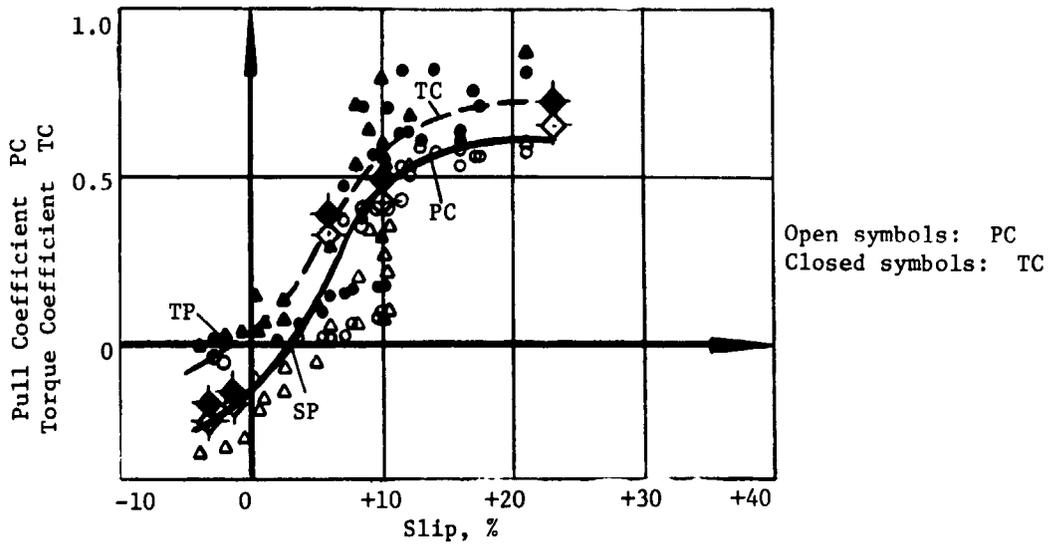
b. Power number as function of pull coefficient and equivalent slope angle (open symbols: $W = 565$ N; closed symbols: $W = 690$ N)

Fig. 11. Performance relations from phase I tests, restrained-pitch mode, soil condition LSS_5

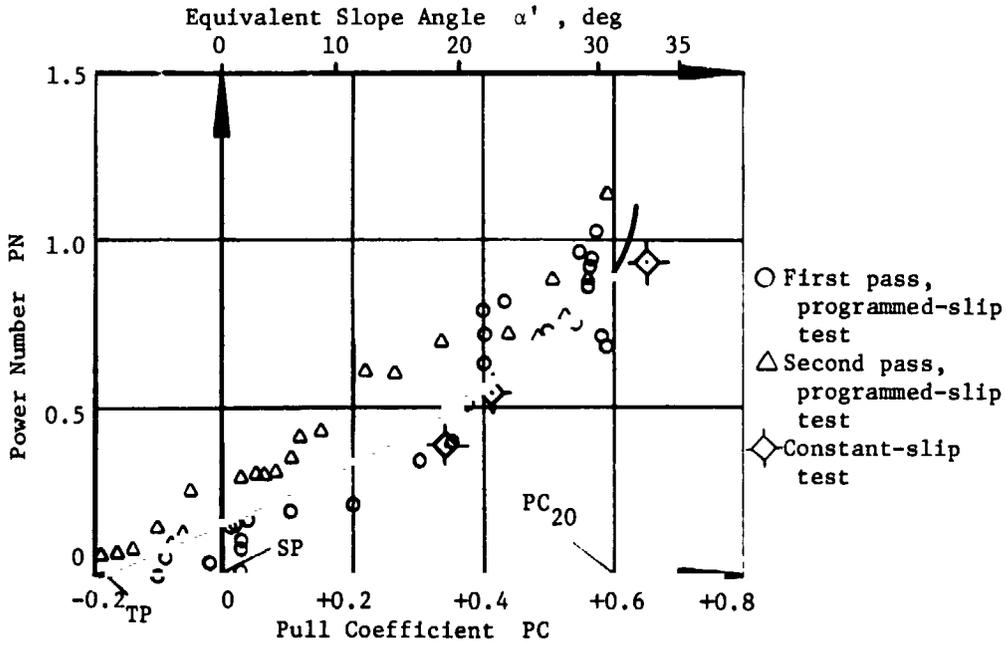
The data obtained from constant-slip tests conducted during phase I on LSS_1 were treated together with results from the programmed-slip tests conducted during the acceptance test program.

54. Plots of PC and TC versus slip, and PN versus PC are shown in figs. 12a and 12b for tests on LSS_1 conducted under a free-pitch mode, and a two-pass test conducted during the acceptance test program. Each of the plots for the programmed-slip tests contains about 20-30 data points that were obtained from only one pass of the ELMS on the soil (e.g. circles in fig. 12b). Thus, each point represents a slip condition occurring instantaneously. In contrast to this, each data point obtained from the constant-slip tests represents an average of one slip condition from one pass of the ELMS (paragraph 36) in which the system was tested under a more stable condition than in a programmed-slip test. Therefore, the data points obtained by the constant-slip test technique (flagged squares in fig. 12) have greater "weight" from a statistical viewpoint than the data points obtained by the programmed-slip test technique.

55. The decision to use the constant-slip test technique in this program instead of the programmed-slip was also based on the following considerations. In tests where wheels act as point loads on the soil, the two test techniques lead to practically the same results, and the statistical validity of the programmed-slip tests can be increased by conducting duplicate tests. However, with a running gear like the ELMS, which has a long contact surface, the point where a certain slip occurs during a programmed-slip test is relatively difficult to define. Generally, this point is assumed to be the geometric center of the running surface. This, of course, is debatable and may be part of the reason for the data scatter in the results from the programmed-slip tests. In contrast to this, during a constant-slip test with the ELMS, the slip conditions are well defined during the entire test run because the slip is constant. Nevertheless, comparison of constant-slip test data with the results of a few programmed-slip tests conducted during the acceptance test program seems justified, since they may be useful in identifying trends.



a. Pull and torque coefficients as functions of slip



b. Power number as function of pull coefficient and equivalent slope angle

Fig. 12. Performance relations from constant-slip tests (phase I) and programmed-slip test (acceptance test No. A-72-001-6), free-pitch mode, soil condition LSS₁, drum rpm ≈ 33, W = 565 N

56. Relations similar to those in fig. 12 are displayed in fig. 13 for tests on LSS₁ conducted under a restrained-pitch mode. Again, the results from programmed-slip tests and constant-slip tests were plotted together and used to establish these relations. The influences of soil condition, pitch mode, loading conditions, and speeds on the performance of the ELMS operating as a single unit on level ground are discussed in paragraphs 62-70.

57. Constant-pull test technique. A method slightly different from that used for phase I data was used to determine the basic performance parameters (PC, TC, and PN) for phase II data (ELMS-trailer configuration on slopes). In phase I, pull and load were continuously measured directly during the test, but during phase II the same values had to be modified to take into account the effects of the trailer, slope angle, load transfer, etc. Basically, two pitch modes had to be considered: free and restrained. In the free-pitch mode the three primary performance parameters were:

$$\underline{a.} \quad PC = P/W_N = (1/W_N)(P_\alpha + P_{TR} + P_a) = \tan \alpha' \quad (5)$$

where

P = total pull developed

W = ELMS weight = constant 690 N

$W_N = W \cos \alpha$ = component of ELMS weight acting normal to the slope surface.

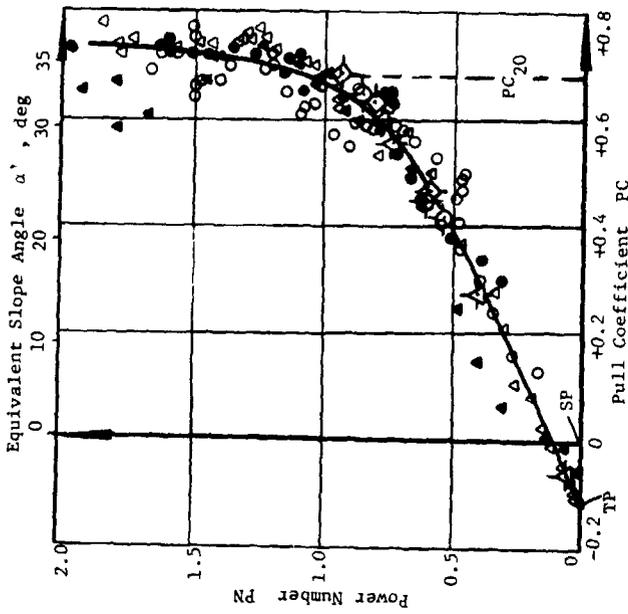
α = angle of the actual slope the system is climbing

$P_\alpha = W \sin \alpha$ = component of ELMS weight acting parallel to the slope in downward direction

$P_{TR} = W_{TR} \cdot \sin \alpha$ = component of the trailer weight acting parallel to the slope in downward direction (W_{TR} = constant 120 N)

P_a = pull applied to the ELMS-trailer system (paragraph 40)

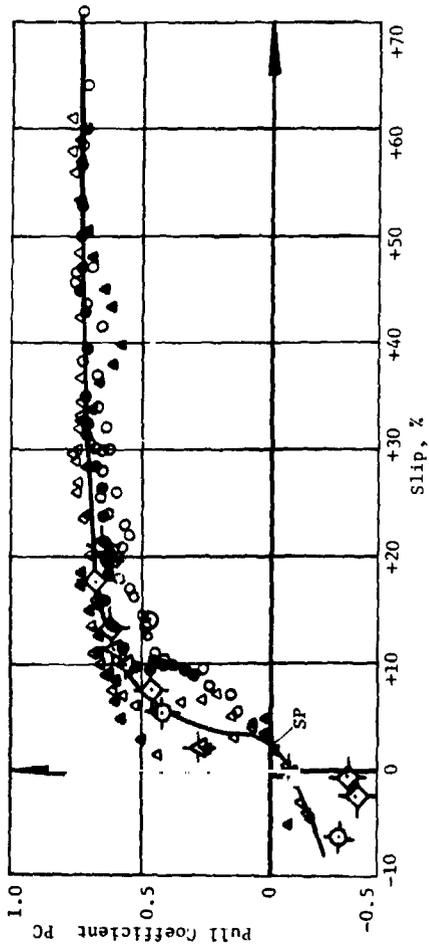
α' = angle of equivalent slope the system would have climbed at the same slip and same power input if part of PC had not been used to overcome P_{TR} and P_a



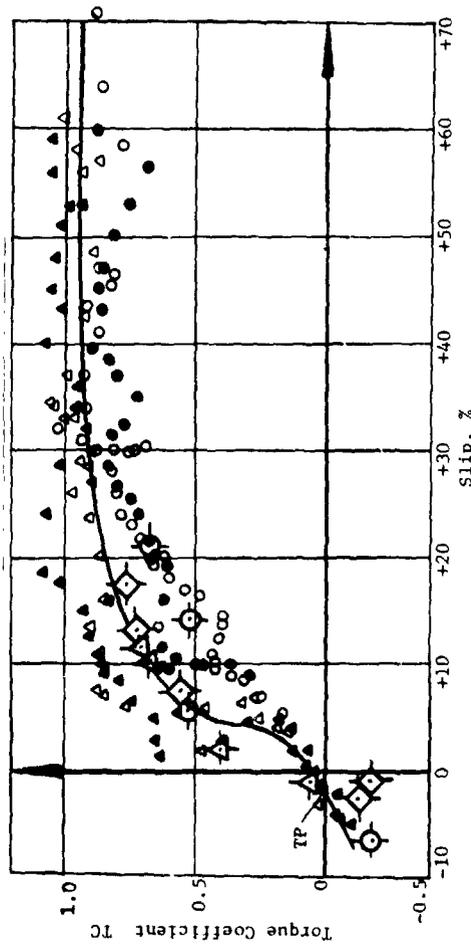
c. Power number as function of pull coefficient and equivalent slope angle

LEGEND

Programmed-Slip Tests (W = 565 N)	Constant-Slip Tests W, N	Pitch Angle, deg
○	Test No. A-72-002-6	565
△	Test No. A-72-005-6	690
○	Open symbols: first pass	565
○	Closed symbols: second pass	+4



a. Pull coefficient as function of slip



b. Torque coefficient as function of slip

Fig. 13. Performance relations from constant-slip tests (phase I) and programmed-slip tests (acceptance tests Nos. A-72-002-6 and A-72-005-6), restrained-pitch mode, soil condition LSS₁, drum rpm ≈ 33.

$$\underline{b.} \quad TC = M/W_N r_e \quad (6)$$

$$\underline{c.} \quad PN = M\omega/W_N v_a \quad (7)$$

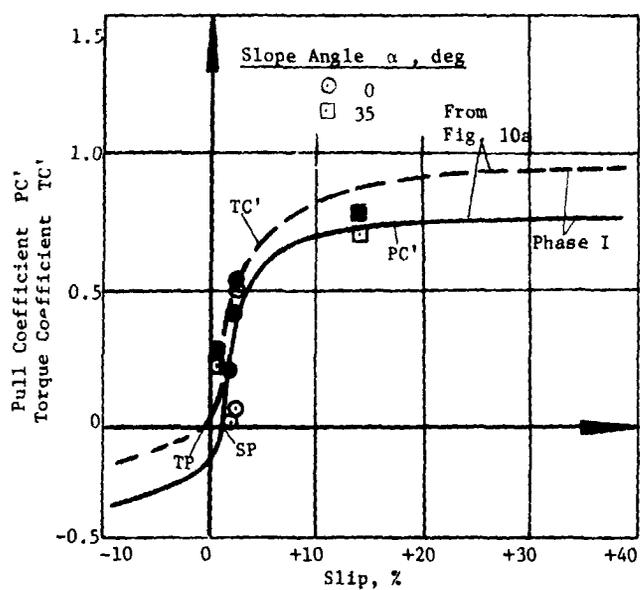
58. When the trailer was rigidly connected to the ELMS (paragraph 29), part of the force component, W_N , was transferred to the trailer. This part, L , was calculated from the measured pitch moment, M'_p , by dividing the latter by the distance from the trailer axle to the point where the trailer arms were connected to the ELMS chassis ($b - a$ in fig. 4b): $L = M'_p / (b - a)$. The pull coefficient PC' corrected for this load transfer, with the system output P being the same, then becomes: $PC' = P/W' = P/(W_N - L)$. Correspondingly, TC' and PN' are: $TC' = M/W' r_e$ and $PN' = M\omega/W' v_a$, respectively).

59. The performance relations from the results of the tests conducted under free-pitch mode on LSS_5 are shown in fig. 14 and for the restrained-pitch mode (fully restrained as well as elastically restrained) in fig. 15. All data shown represent conditions in which the ELMS-trailer system was not stalled. The influence of pitch mode on the performance is discussed in paragraphs 72-77.

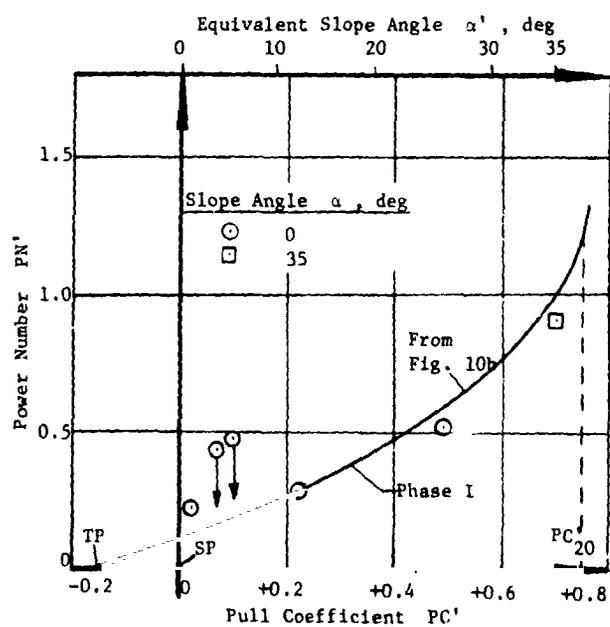
60. Programmed-pull test technique. The results of only one such test, which was conducted under fully restrained-pitch mode on LSS_1 (paragraph 44), were used in the analysis. Therefore, the results are presented in the overall analysis of the tests conducted on slopes (paragraph 78).

Phase III: Miscellaneous tests

61. Representative torque and distance records for obstacle-surmounting and crevasse-crossing tests are given in the discussion of the test results (paragraphs 83 and 84); therefore, no typical relations are presented at this point. Peak torques for these tests are listed in table A7. Also, the results of tests to evaluate the internal losses and to determine the contact pressure distribution of the ELMS are presented in the analysis of the data (paragraphs 85-87 and 88, respectively).

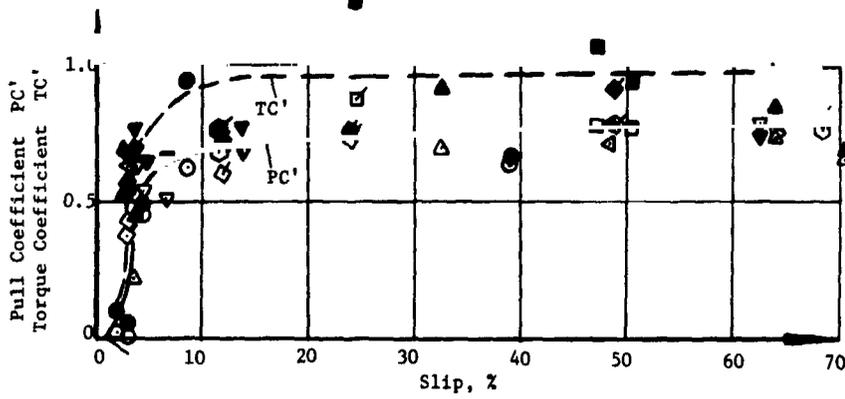


a. Pull and torque coefficients as functions of slip (open symbols: PC'; closed symbols: TC')

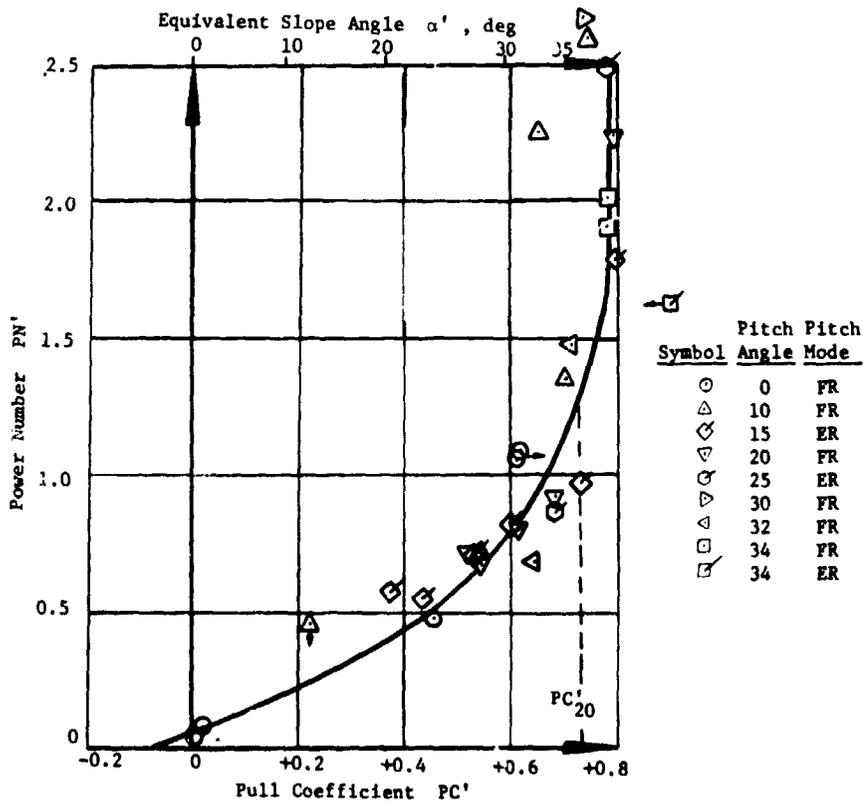


b. Power number as function of pull coefficient and equivalent slope angle

Fig. 14. Performance relations from phase II tests, free-pitch mode, soil condition LSS₅



a. Pull and torque coefficients as functions of slip (open symbols: PC'; closed symbols: TC')



b. Power number as function of pull coefficient and equivalent slope angle

Fig. 15. Performance relations from phase II tests, restrained-pitch modes, soil condition LSS₅ (FR = fully restrained pitch; ER = elastically restrained pitch)

PART IV: ANALYSIS OF TEST RESULTS

Soft-Soil Performance

Performance on level ground (phase I)

62. Influence of load. The dependence of the pull and torque coefficients PC and TC, and power number PN on the applied load, for the load range (565-690 N) used in these tests, can be ascertained from figs. 10-13. Accordingly, within the usual experimental data scatter, which is expected from mobility performance tests on relatively soft soil, PC, TC, and PN appear to be independent of the applied load, regardless of variations in other test conditions, i.e. soil consistency (LSS_1 and LSS_5), pitch mode (free or restrained), and ELMS speed. These conclusions correspond qualitatively to the findings of a study conducted by Freitag, Green, and Melzer (1970) on several wheel concepts for lunar roving vehicles. On the basis of that study, it was found that a change in load did not influence the performance of the running gears as long as their contact pressure was equal to or less than about 3.5 kPa. Under the two loads tested in this study, the mean contact pressure of the ELMS was about 2.1 and 2.8 kPa, respectively (paragraph 88 and figs. 28 and 29).

63. Influence of ELMS drum rpm. Figs. 10b and 11b also contain data points from a few tests conducted at a prescribed test drum rpm of 130, which resulted actually in an average rpm of 100 and a translational velocity of the drums of about 1.5 m/sec (paragraph 36). An rpm of 100 is about three times the average of 0.5 m/sec (33 rpm) at which the majority of the tests were conducted. The high-speed data fall well within the general data scatter, indicating that over the range tested the ELMS performance was not influenced by a change in drum rpm or in translational speed of the loop. This behavior pattern was also observed when wire-mesh wheels were tested on the same soil and must be attributed to the fluid permeability characteristics of the lunar soil simulant (development of pore air pressure at higher speeds; see Melzer, 1971).

64. Influence of pitch mode. To determine the influence of pitch on performance, the free-pitch angles (β) of the ELMS with the horizontal

were plotted versus slip for each test conducted in a free-pitch mode (fig. 16). These data show that the ELMS was traveling at a negative pitch angle (nose-down position) in the negative slip range; at zero slip, the pitch angle was also zero. At positive slip values, pitch was also positive (nose-up position), and β increased with increasing slip. From these results, it was hypothesized that performance would be increased if the pitch angles were restrained to angles smaller than about 4 deg. This hypothesis appeared justified, because under a free-pitch mode, the ELMS running surface tended to lose contact with the soil as slip and pitch angle increased (see figs. 3a, 3b, and 4a, the latter showing the ELMS on a slope where the same phenomenon was observed); whereas under restrained pitch ($\beta \leq 4$ deg), a better contact between the traction elements and the soil resulted, causing the load to be distributed over a larger area which, in turn, tended to mobilize a greater thrust from the soil (see figs. 4b and 4c; $\beta \approx 0$ deg). Thus, at a given slip, better performance would result for restrained-pitch mode than for free pitch. Furthermore, the towed force (negative slip) at a zero or positive restrained-pitch angle would tend to be smaller in magnitude than that developed under free pitch (negative pitch angle; nose-down position) because the nose of the system would actually be lifted up if the ELMS were restrained. This lifting would lead to a more favorable load distribution and a decrease in surface traction; thus, the force required to tow the system would decrease.

65. These general expectations were confirmed by results of tests on both dense and loose soil (fig. 17). (The relations shown in fig. 17 were taken from figs. 10b, 11b, 12b, and 13c.) For both soil conditions, the system output (PC) was larger at a given power input when the ELMS was restrained. Characteristic performance parameters for the two pitch modes and the two soil conditions are also listed in table 4. These parameters are: towed force coefficient PC_T , power number for the self-propelled condition PN_{SP} , and power number PN for a given system output PC .

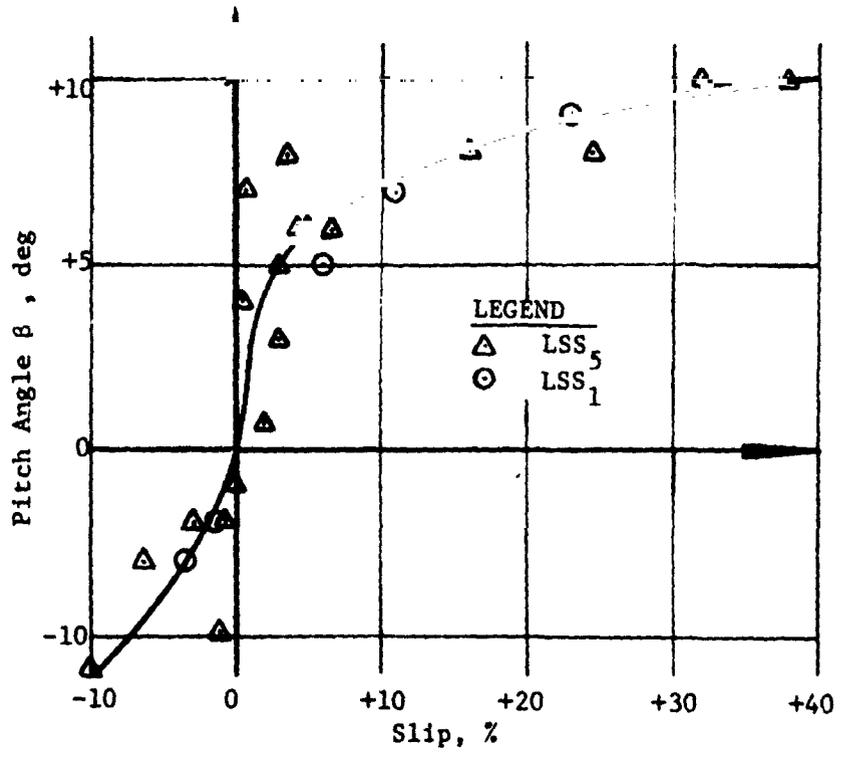


Fig. 16. Relation of pitch angle β to slip from tests with ELMS II in free-pitch mode

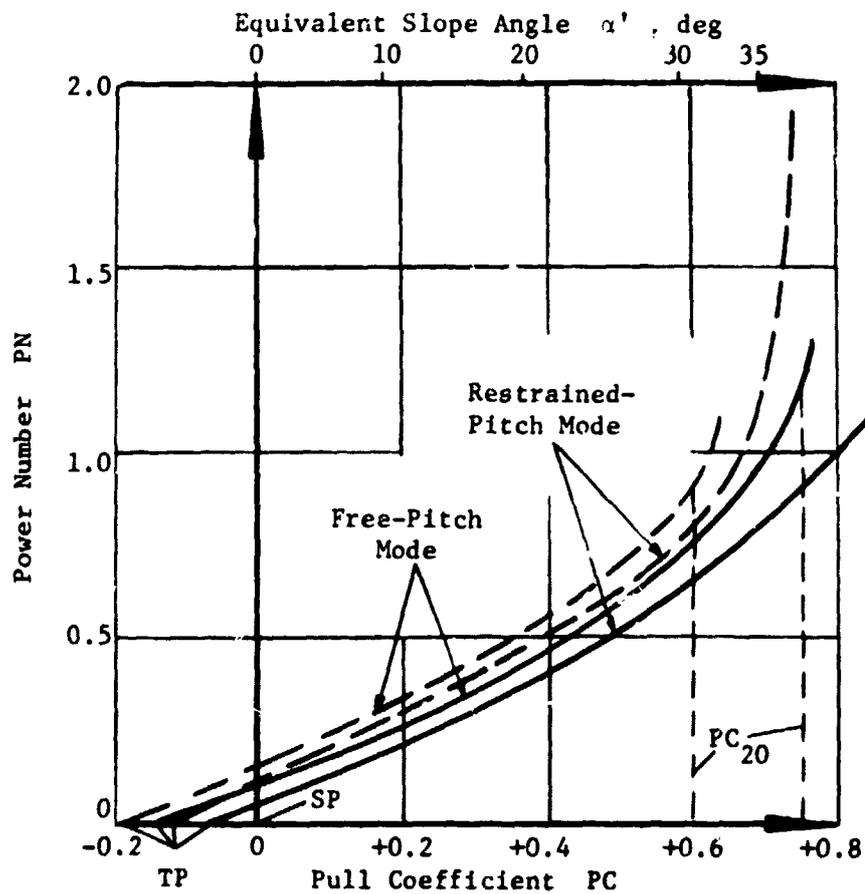


Fig. 17. Summary of PN versus PC relations developed from tests on level ground (phase I, figs. 10-13), soil conditions and pitch modes tested (solid lines: LSS₅; dashed lines: LSS₁)

Table 4

Soil Condition	Pitch Mode	PC_T	PN_{SP}	$PN \leftrightarrow PC^*$
LSS ₅	Free	0.13	0.09	1.18 ↔ 0.75
	Restrained	0.07	0.06	0.91 ↔ 0.75
LSS ₁	Free	0.19	0.16	0.92 ↔ 0.60
	Restrained	0.12	0.11	0.80 ↔ 0.60

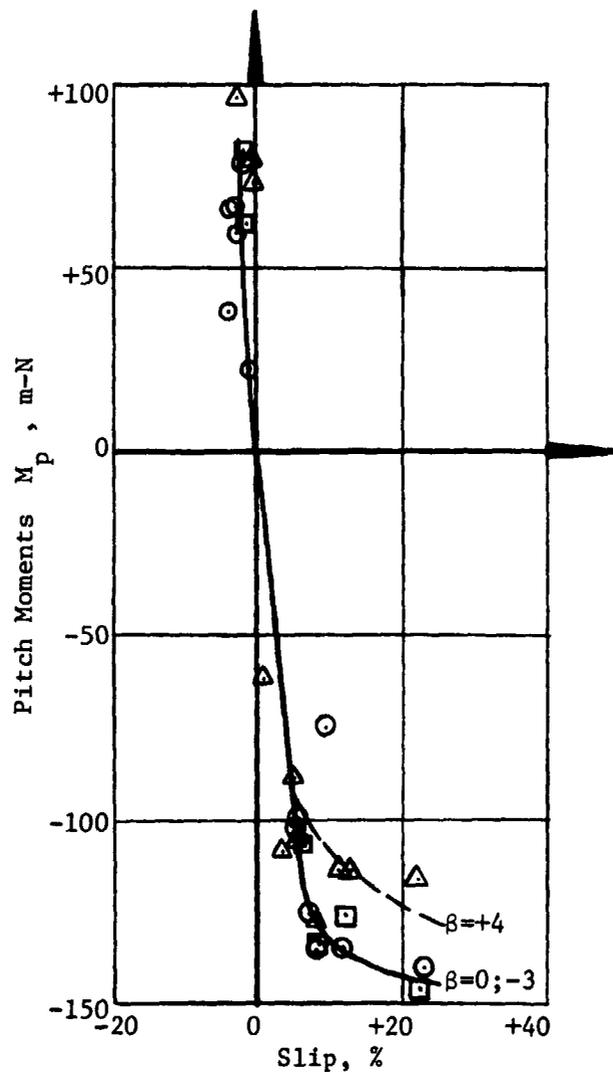
* Corresponds to PC measured at 20 percent slip for free-pitch mode; see fig. 17.

66. As shown in figs. 11b, 13c, and 17, the PN versus PC relation under a restrained-pitch mode is essentially independent of pitch angles for pitch angles β of -3, 0, and +4 deg.

67. Fig. 18 shows the dependence of the restrained-pitch moment (M_p) on slip as obtained from tests conducted on LSS₅.^{*} At negative slips and at positive slips smaller than about 5 percent, M_p appears to be independent of the restrained-pitch angle β and to increase in magnitude with increasing slip. However, at slips larger than about +5 percent, the absolute values of the pitch moment appear to decrease with increasing pitch angle, presumably because β tends to approach the equilibrium angles that would be developed in free-pitch condition (see fig. 16).

68. Influence of soil strength. Table 4 and the average relations in fig. 17 indicate the influence of soil strength on performance. For a given pitch mode, the towed force coefficients PC_T and the power requirements PN_{SP} are larger on LSS₁ (loose soil) than on LSS₅ (dense soil), as one would expect. This holds true for all values of PC or α' . Fig. 17 indicates further that the maximum pull coefficient PC, hence angle α' of equivalent slope, that can be developed without excessive power requirements (stable system output) is larger for LSS₅ than for LSS₁.

* Only results of tests conducted on LSS₅ are used here because the majority of the slope tests (phase II) were conducted on LSS₅. The M_p values of phase I will be compared later (paragraph 81) with corresponding values of phase II. Additional results of phase I for LSS₁ are listed in tables A3 and A4.



Pitch Angle	
β , deg	
⊙	0
△	+4
□	-3

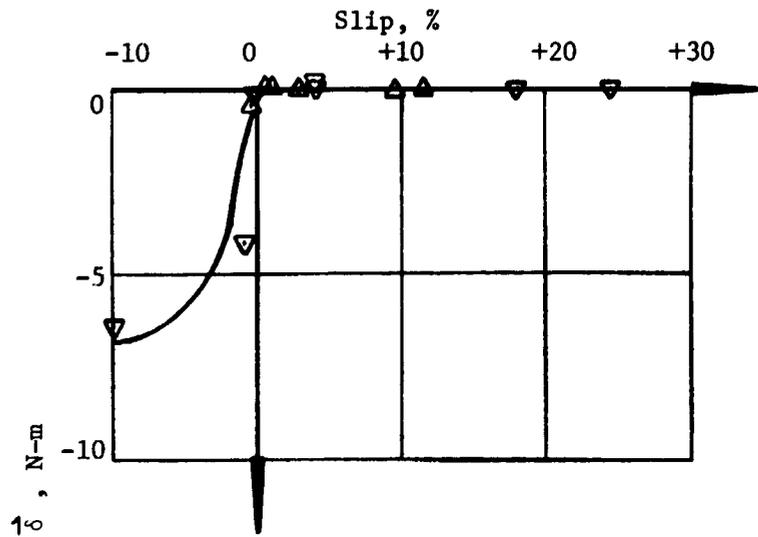
Fig. 18. Pitch moments from restrained-pitch tests on level ground (phase I) on soil condition LSS₅

69. Shock absorber performance. Only a qualitative evaluation of the performance of the shock absorbers was made within the framework of this program. Only data from tests (constant-slip) conducted on LSS₅ under a free-pitch mode are presented here. Additional data from tests on LSS₁ and restrained-pitch tests are listed in tables A3 and A5.

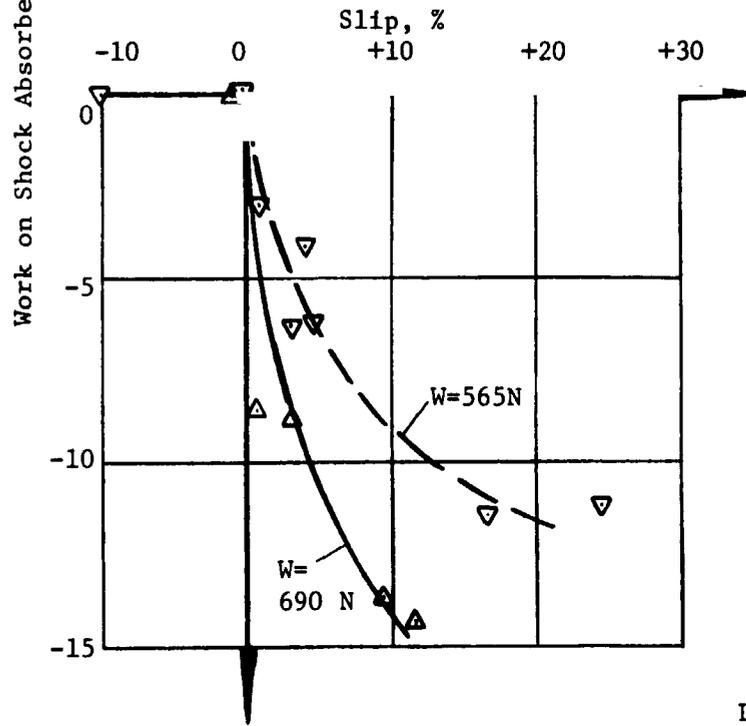
70. During each test, the force \vec{F} exerted by the suspension arms of the ELMS (fig. 1) displaced the shock absorber piston in a single stroke. This displacement δ , which depends on the pitch angle, remained constant for the duration of the test, because the pitch angle did not change during a constant-slip test. The dot product $\vec{F} \cdot \vec{\delta}$ was used to describe the work on the shock absorbers under the various test conditions ($\vec{F}_f \cdot \vec{\delta}_f$ for the front and $\vec{F}_r \cdot \vec{\delta}_r$ for the rear shock absorbers). The following sign convention was used: $\vec{F} \cdot \vec{\delta}$ was negative in case of compression of the shock absorber; $\vec{F} \cdot \vec{\delta}$ was positive in case of tension. As fig. 19a indicates, the front shock absorber was compressed (negative $\vec{F}_f \cdot \vec{\delta}_f$) when slip was negative. This was expected because of the nose-down position of the system in the negative slip range (fig. 16). In the same slip range, however, $\vec{F}_r \cdot \vec{\delta}_r$ was practically zero (fig. 19b), indicating that the rear shock absorber did not have to fulfill any damping requirements. The reverse situation occurred in the positive slip range, i.e. the rear shock absorber was compressed (nose-up position) and $\vec{F}_r \cdot \vec{\delta}_r$ increased negatively with increasing slip (fig. 19b), while $\vec{F}_f \cdot \vec{\delta}_f$ was zero. In addition, $\vec{F}_f \cdot \vec{\delta}_f$ seemed to be influenced by the ELMS load; at a given positive slip, the absolute value of $\vec{F}_f \cdot \vec{\delta}_f$ was larger for a load of 690 N than for a load of 565 N. In paragraph 82 (fig. 24), these relations are compared in a normalized form with the corresponding relations obtained from the slope tests (phase II).

Performance on slopes (phase II)

71. Influence of ELMS drum rpm and load. Because no influence of drum rpm on performance was noted during the phase I tests (paragraph 63),



a. Front shock absorber



b. Rear shock absorber

LEGEND
Load W , N
△ 690
▽ 565

Fig. 19. Relations between $\vec{F} \cdot \vec{\delta}$ and slip for front and rear shock absorbers, free-pitch mode, LSS₅, phase I tests

only a few check tests were conducted during phase II at high rpm (130), indicating again no apparent dependence of performance on rpm. Accordingly, no distinction is made hereafter between data from tests conducted at low and high rpm's. The dependence of ELMS performance on load was checked in a similar manner. With slope angles ranging between 0 and 35 deg and the deadweight of the ELMS being 690 N, the range of forces acting perpendicular to the slopes tested was covered during phase I by the minimum load of 565 N and the maximum load of 690 N. Within this range no influence of load on performance was noted (paragraph 62). Thus, if any difference between performances (PN, PC) on level ground and on slopes had been found, it could not have been attributed to a difference in the magnitude of loads.

72. Influence of pitch mode. Because only one test was conducted on LSS₁, the analysis that follows concentrates mainly on results of tests conducted on LSS₅. These results are shown in figs. 14 and 15.

73. Before going into more detailed analysis, the following simplification can be made. The unflagged symbols in fig. 15b indicate results from tests conducted in fully restrained pitch, and the flagged symbols indicate results from tests conducted in elastically restrained pitch.* However, the general trend of the data does not show a distinct difference between the two restrained-pitch modes, and they can be represented by a single relation between power requirements and system output within the experimental data scatter. For these reasons, these two pitch modes will be referred to hereafter as restrained-pitch mode.

74. The maximum angles of the slopes that could be negotiated by the ELMS in free-pitch and in restrained-pitch modes (from tables A5 and A6) are compared in table 5.

* It was hoped that in the elastically restrained condition the ELMS would be allowed to pitch at a small angle. Actually, very little pitch motion was observed during the tests in this condition (fig. 4c), because of the relatively large stiffness of the coil springs (paragraph 29) provided by LMSC.

Table 5

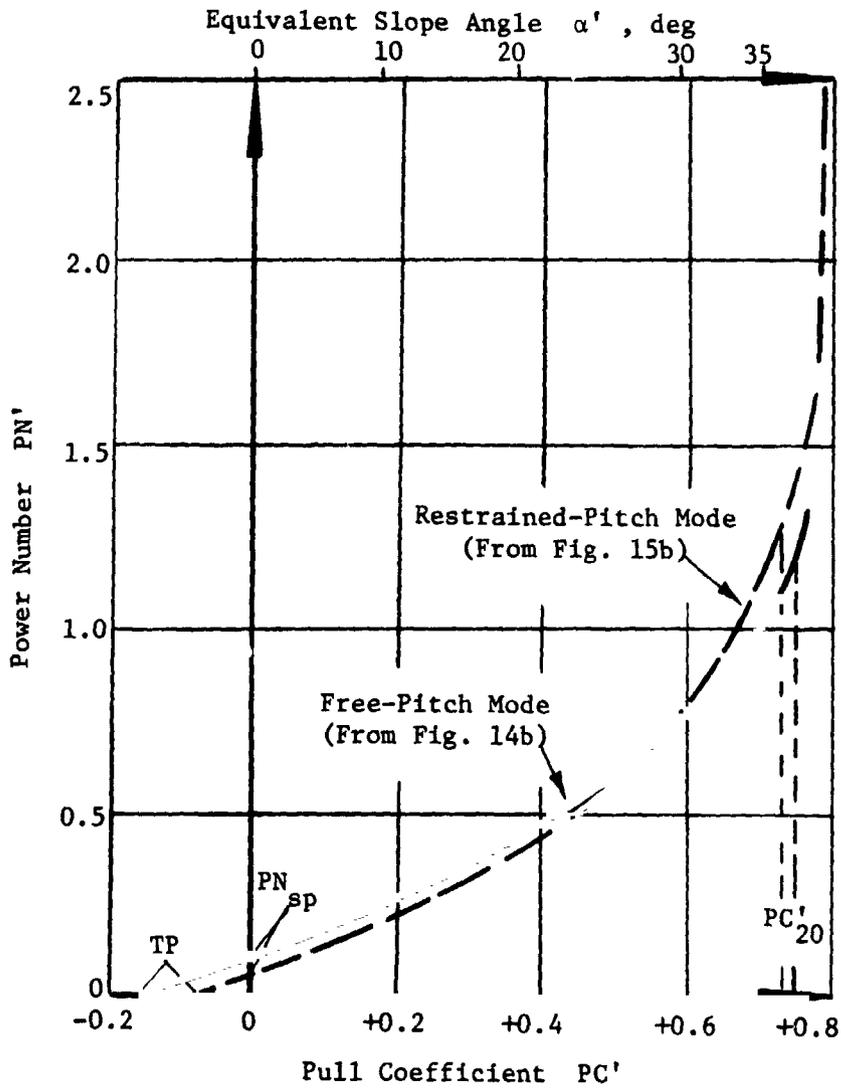
<u>Test No.</u>	<u>Pitch Mode</u>	<u>Actual Slope Angle α_{\max}, deg</u>	<u>PC</u>	<u>Equivalent Slope Angle α'_{\max}, deg</u>	<u>PC'</u>
016-6, Pass 1	Free	35	0.70	35.0(= α)	0.70 (=PC)
016-6, Pass 2	Restrained	34	0.68	37.6	0.77
016-6, Pass 3	Restrained	34	0.68	42.0	0.90
0.13-6	Restrained	34	0.68	37.9	0.78

In terms of the angle (α) of the slope actually climbed by the system, table 5 shows that the ELMS performed better when operated in a free-pitch mode than in restrained pitch. However, if the influence of load transfer (paragraph 58) is taken into account in the evaluation of the ELMS performance on slopes under a restrained-pitch mode, the resulting values of equivalent slope angle (α') indicate that the system performed better when operated in a restrained-pitch mode.* One would also expect this result from the phase I tests on level ground (paragraph 65).

75. Next, comparison was made between the power requirements for the two pitch modes over the full range of system output (PC'). For this purpose, the relation from fig. 14b (free pitch) was plotted in fig. 20, together with the relation from fig. 15b (restrained pitch). Fig. 20 indicates a slightly better performance under a restrained-pitch mode up to PC' values of about 0.5 to 0.6 (less power required at a given PC'). For higher PC' values, power requirements are less under a free-pitch mode. However, as shown in the foregoing paragraph, theoretically the ELMS can potentially climb a steeper slope if it is restrained from pitching.

76. This behavior is somewhat contrary to the observations made

* The effect of load transfer occurring as a result of pitch restraint can be avoided by attaching to the existing ELMS a trailing or leading powered ELMS unit with a pitch-locking mechanism.



NOTE: $PC' = PC$ and $PN' = PN$ for free-pitch mode during which no load transfer takes place.

Fig. 20. Comparison of performance relations for free-pitch mode and restrained-pitch mode on slopes, phase II tests, soil condition LSS_5

concerning the influence of the pitch mode on the level-ground performance of the ELMS operating in the dynamometer system (phase I, paragraph 65). The differences will be discussed when the results of both testing modes (phases I and II) are compared (paragraphs 79-81).

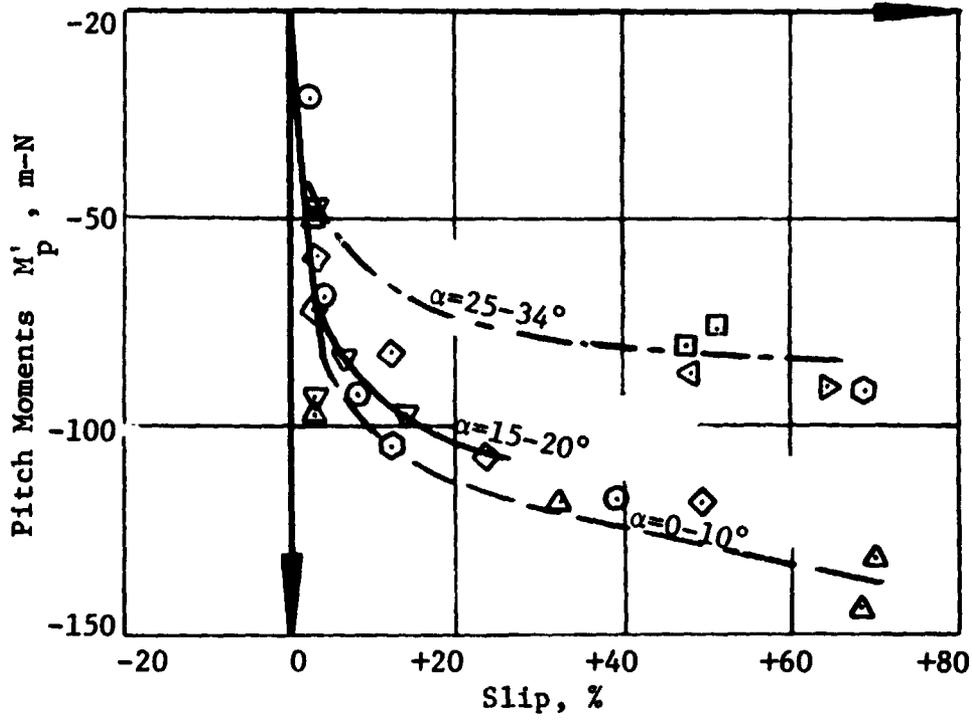
77. To ascertain the variation in magnitude of the pitch moment (M'_p) that occurred during the tests in restrained-pitch mode, M'_p values were plotted versus slip (fig. 21). At very low positive slip (<+3 percent), the relation can be represented by a single curve showing an increase of pitch moment with increasing slip. At larger slips, the data indicates that the pitch moment M'_p increases with increasing slope angle α . The values of M'_p appear to be proportional to the load component acting perpendicular to the slope surface, which also decreases with increasing slope angle (see paragraph 81).

78. Influence of soil strength. Pertinent comparisons can be made from the data listed in table 6. Because only one test conducted on LSS₁ could be used in the analysis, and this test was conducted under a restrained pitch mode on the maximum actual slope climbed, only the corresponding maximum actual slope/restrained pitch conditions on LSS₅ were used in table 6.

Table 6

<u>Test No.</u>	<u>Soil Condition</u>	<u>Actual Slope Angle α_{max}, deg</u>	<u>PC</u>	<u>Equivalent Slope Angle α'_{max}, deg</u>	<u>PC'</u>
009-6 Pass 2	LSS ₁	27	0.60	34.6	0.69
016-6, Pass 2	LSS ₅	34	0.68	37.6	0.77
016-6, Pass 3	LSS ₅	34	0.68	42.0	0.90
013-6	LSS ₅	34	0.68	37.9	0.78

As one would expect from the tests on level ground (phase I, paragraph 68), α_{max} , as well as α'_{max} , is smaller for the softer soil (LSS₁) than for the firmer soil (LSS₅).



LEGEND
Slope Angle α , deg

- 0
- △ 10
- ◇ 15
- ◁ 20
- ◉ 25
- ◓ 30
- ◔ 32
- ◻ 34

Fig. 21. Pitch moments as functions of slip from tests under restrained-pitch mode on slopes, phase II tests, soil condition LSS₅

Comparison of ELMS performance
on level ground (phase I) with
performance on slopes (phase II)

79. To determine whether the slope-climbing capability of the ELMS can be predicted from results of tests conducted on level ground, phase I and phase II test results were compared, as indicated in fig. 14. Since the same performance relations for free-pitch mode on LSS_5 can be used to display the results of phase I and phase II tests, the slope-climbing capability (in terms of PC, PN, and α') can be predicted from level-ground tests if the ELMS is operating in the free-pitch mode.

80. The average trends of the plots of PN versus PC for free-pitch mode, obtained from fig. 14, are plotted in fig. 22. The same figure also contains average trends from PN versus PC plots from data obtained from phase I tests (fig. 11b) and phase II tests (fig. 15b) conducted under a restrained-pitch mode. For PC' values smaller than about 0.4, corresponding to an equivalent slope angle of about 22 deg (point "A" in fig. 22), the relations from phases I and II for the restrained pitch mode are essentially the same. For larger PC' values, the power requirements for a given system output are higher for the system operating on slopes (phase II) than for the system in the dynamometer carriage operating on level ground (phase I). This means that the slope-climbing capability of the ELMS when restrained in pitch can be predicted from level-ground tests only for PC' smaller than 0.4. In addition, for pull coefficient values larger than 0.5, the ELMS performance on level ground (phase I) was more efficient (lower energy requirements at a given PC value) under restrained pitch conditions than under a free-pitch mode; however, the reverse trend was indicated for PC' values larger than 0.5. The ELMS performance on slopes under restrained pitch conditions was less efficient than it was under a free-pitch mode on either level ground or slopes. On the other hand, the maximum slope-climbing capability of the system indicated under a restrained pitch mode ($\alpha' = 38$ deg) was higher than that indicated under free-pitch mode ($\alpha' = 35$ deg).

81. An attempt was made to normalize the pitch moments measured

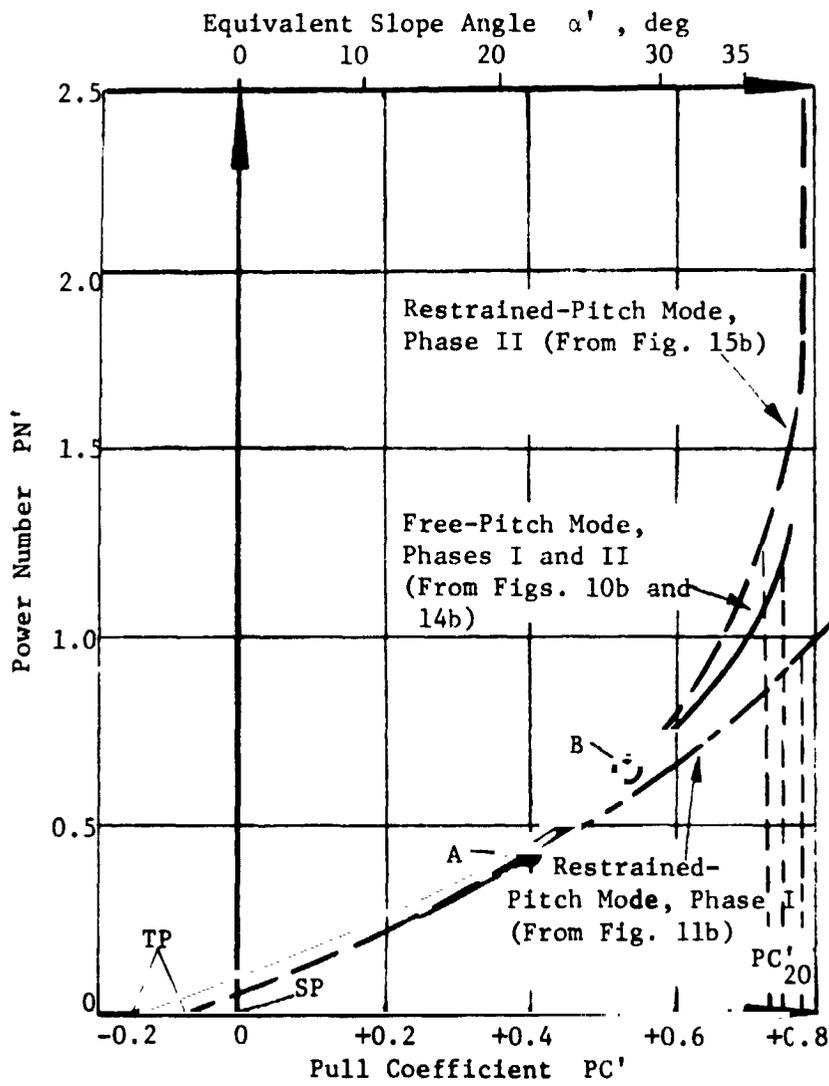


Fig. 22. Comparison of performance relations for various pitch modes with ELMS II operating on level ground (phase I) and on slopes (phase II), soil condition LSS_5

during the two testing phases. For this purpose, the pitch moments measured in phase II were recalculated as if they had been measured at the center point of the ELMS, i.e. the same point at which they had been measured during phase I. In addition, they were normalized for the influence of load W' acting perpendicular to the slope:

$$\frac{M_p}{W_N} = \frac{M'_p \cdot b}{d \cdot W'} \quad (8)$$

where

M_p, M'_p = measured pitch moment

b = distance between center point of ELMS and trailer axle = 1.42 m

$d = b - a$ - a distance between trailer axle and connecting point at ELMS = 1.07 m; $b = 1.42$ m, $a = 0.35$ m (see fig. 4b)

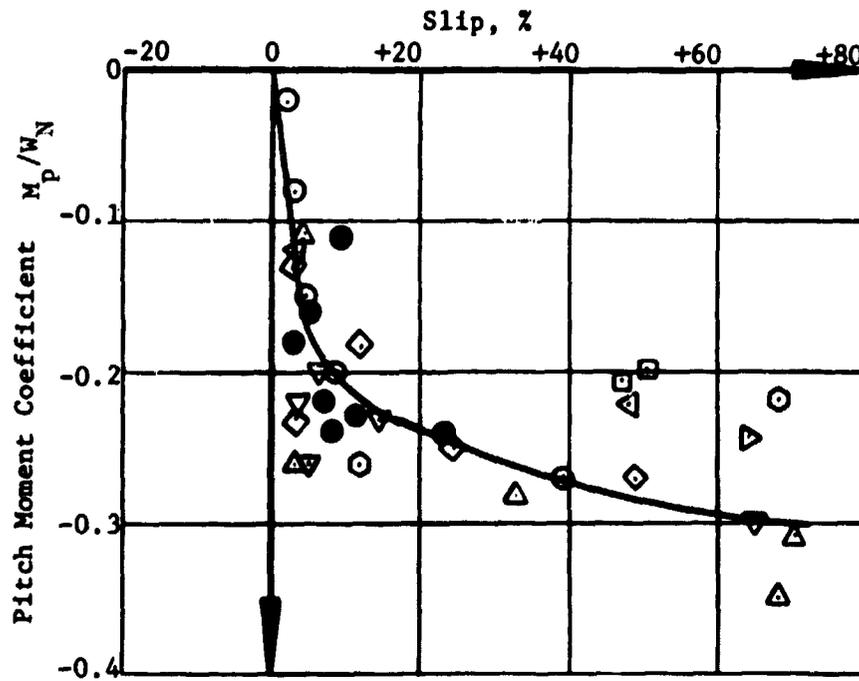
W_N = normal load (no load transfer taking place; phase I tests)

W' = normal load (load transfer taking place; phase II tests)

Equation 8 fulfills the requirement that for $d = b$, $M'_p = M_p$, which in this case would have been measured at the center point of the ELMS as it actually was done during phase I. The results of this analysis are shown in fig. 23, where M_p/W_N is plotted versus slip. Two conclusions can be drawn from fig. 23. First, the separation by slope angle, as observed in fig. 21 for the phase II tests (paragraph 77), is no longer apparent* because the data have been normalized to account for the influence of W' . Secondly, the data from phase I for $\beta = 0$, corresponding to the pitch condition tested in phase II, coincide with the phase II data after the influence of load has been taken into account.

82. The last point to be investigated in this comparison of phase I and phase II test results was the performance of the shock absorbers. As has been mentioned (paragraph 69), only results of free-pitch tests could

* There is still some data scatter at high slips, probably because at high slip rates, the whole system started to vibrate, thus influencing the quality of the pitch moment measurements.



LEGEND

Phase I: $\beta = 0$
 $\alpha = 0$

Phase II: $\beta \approx 0$

Slope Angle α , deg

- 0
- △ 10
- ◇ 15
- ▽ 20
- ⊙ 25
- △ 30
- ▽ 32
- 34

Fig. 23. Pitch moment coefficient as function of slip, phase I and phase II tests, soil condition LSS₅

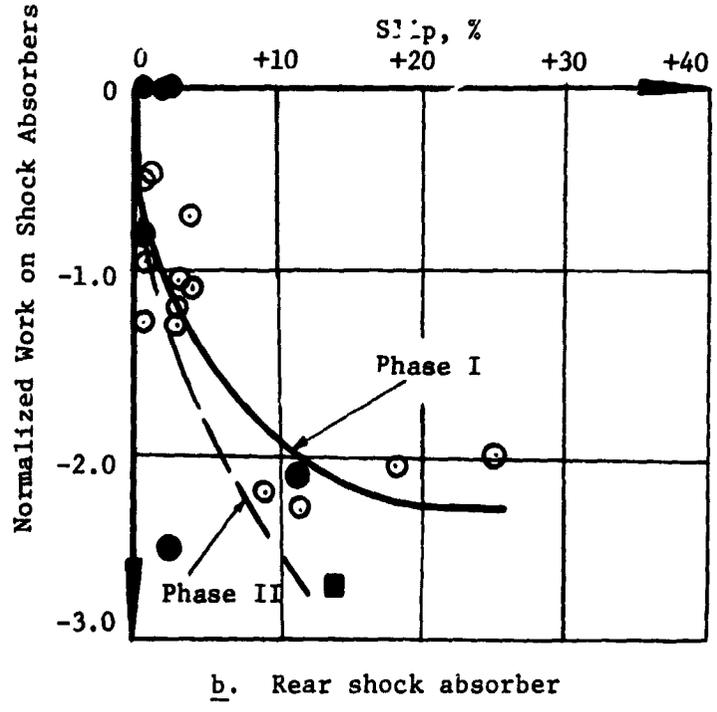
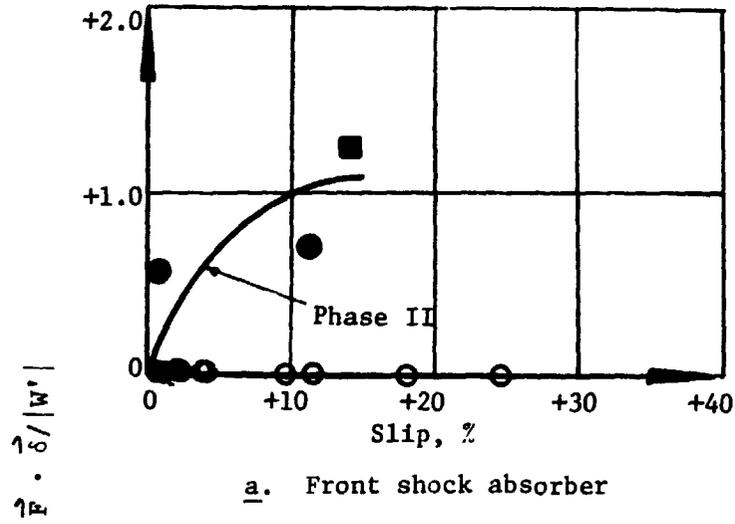
be used. The $\vec{F} \cdot \vec{\delta}$ values were normalized for the influence of load and plotted versus slip (see fig. 24*). The data for the rear shock absorber measured during phase I do not separate by load (compare figs. 19b and 24b), and the shock absorbers show different performances during phases I and II. The $\vec{F} \cdot \vec{\delta}$ for the front shock absorber (fig. 24a), resulting from tension, was positive in the positive slip range during phase II; whereas $\vec{F} \cdot \vec{\delta}$ was zero during phase I tests. Thus, although no difference in performance in terms of PN and PC could be observed between slope tests (phase II) and level-ground tests (phase I) both conducted under a free-pitch mode (see fig. 22), a distinct difference can be noted in the performance of the shock absorbers. This difference was probably caused by the ELMS being mounted at its rear end to the trailer for the phase II tests instead of at its center (higher pitch angle at a given slip than in the case of the phase I configuration).

Obstacle-Surmounting and Crevasse-Crossing Capabilities

Obstacles

83. Results of obstacle-surmounting tests are presented in table A7. The ELMS, in restrained pitch, climbed a 38-cm-high obstacle. However, because the pitch was restrained, the rear end of the ELMS was lifted. The test was stopped at this point, although the system had not surmounted the obstacle for its full length. It was concluded, however, that the ELMS would have easily climbed the obstacle if the system had been supported by a second trailing powered unit. The ELMS in free pitch climbed a 46-cm-high obstacle (figs. 8 and 25); but after it had traveled for about 60 cm (slightly less than one-half its length, see fig. 25), the yoke of the trailer hit the level surface and the test was stopped. The record of torque versus distance traveled for this test (fig. 25) shows relatively uniformly distributed torque requirements for about the first 30 cm of travel (1/5 of the

* Only positive slip is shown because negative slip could not occur during the phase II tests.



LEGEND
Slope Angle α , deg
 ● 0
 ■ 35

Fig. 24. Relations between normalized work on shock absorbers and slip during phases I and II, free-pitch mode
 (open symbols: phase I;
 closed symbols: phase II)

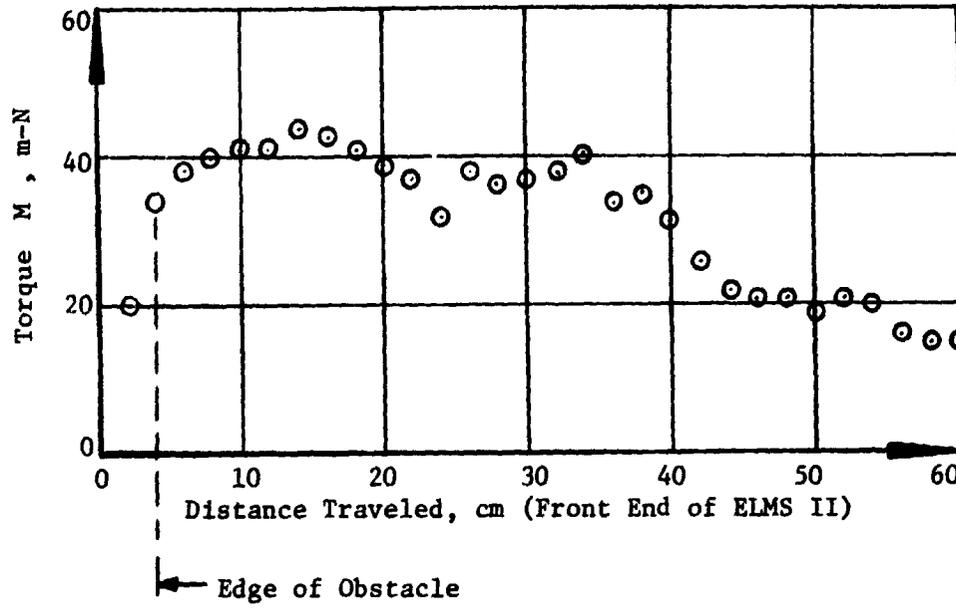


Fig. 25. Torque requirements for ELMS II in free-pitch mode climbing a 46-cm-high obstacle

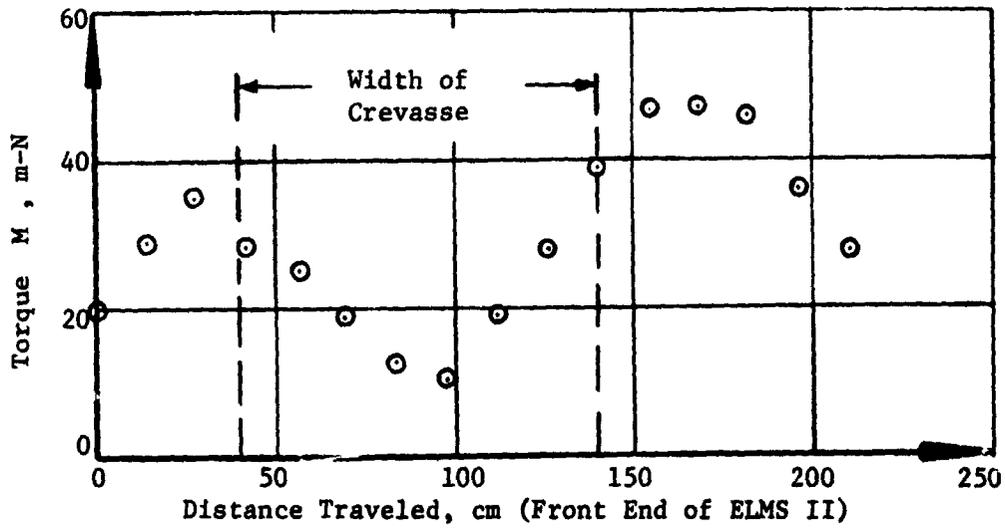


Fig. 26. Torque requirements for ELMS II in free-pitch mode traversing 100-cm-wide crevasse

ELMS length) where the highest traction was required (fig. 8). After this, the critical point in the surmounting process had been overcome, and torque requirements decreased.

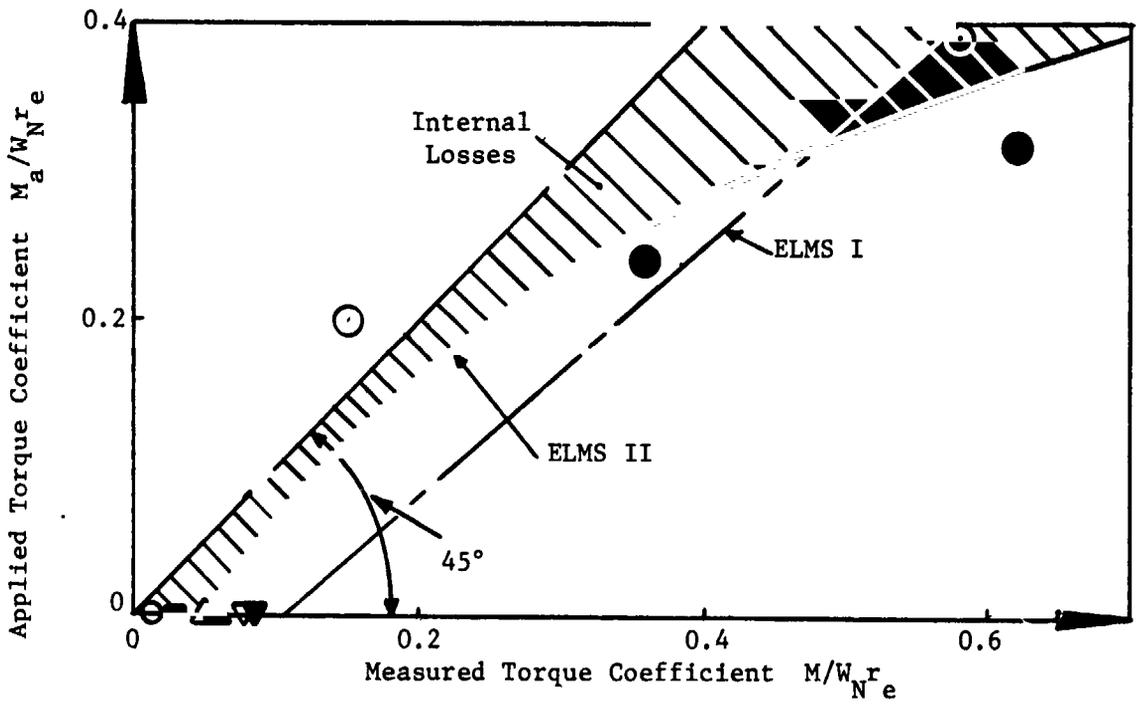
Crevasses

84. Results of crevasse-crossing tests are presented in table A7. The maximum crevasse crossed was 100 cm wide with the ELMS II in free pitch as well as in restrained pitch. A record of torque versus distance traveled by the ELMS is shown in fig. 26. Peak torque was reached after the front end of the system reached the opposite side of the crevasse. As in the obstacle tests, the general impression was that the ELMS would definitely be able to cross wider crevasses if the system were supported by a second powered unit connected with controlled pitch to the leading unit.

Evaluation of Internal Losses

85. Measured torque coefficients ($M/W_{N_e}r_e$) versus torque coefficients calculated from the externally applied torques ($M_a/W_{N_e}r_e$) (paragraph 48) are shown in fig. 27. The internal losses for a specific measured torque are given by the difference between $M/W_{N_e}r_e$ and $M_a/W_{N_e}r_e$; they increase with increasing $M/W_{N_e}r_e$. The influence of drum rpm was checked at $M_a/W_{N_e}r_e = 0$, but no dependency on rpm was noted for the range tested (16 to 97 rpm).

86. The corresponding relation evaluated for the ELMS I (Melzer and Green, 1971) is also shown in fig. 27. In contrast to the relation established for the ELMS II, the relation for the ELMS I is linear. It intersects the former at an $M/W_{N_e}r_e$ value of about 0.5. Table 7 shows some values of internal losses for both systems at certain externally applied torques.



Drum RPM

- ⊙ 16
- △ 32
- 65
- ▽ 97

Open symbols: $W = 565$ N
 Closed symbols: $W = 690$ N

Fig. 27. Relation between applied and measured torque coefficients for evaluation of internal losses

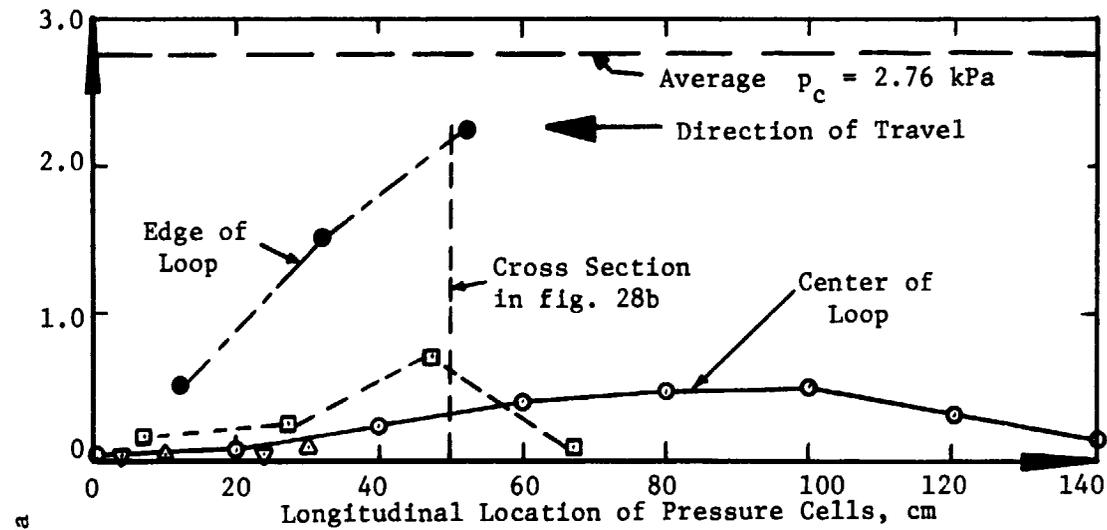
Table 7

$M_a/W_{N_e}^r$	$M/W_{N_e}^r - M_a/W_{N_e}^r$	
	ELMS I	ELMS II
0	0.11	0.05
0.20	0.15	0.06
0.30	0.18	0.15
0.40	0.20	0.34

87. Generally, the relations displayed in fig. 27 can be used for qualitative comparisons; for example, to compare the internal losses of the two systems (ELMS I and II) as in the foregoing paragraph. However, the absolute values are too high, probably because of the inadequacy of the test setup (load simulations, vibration of the system, etc.; see also Melzer and Green, 1971).

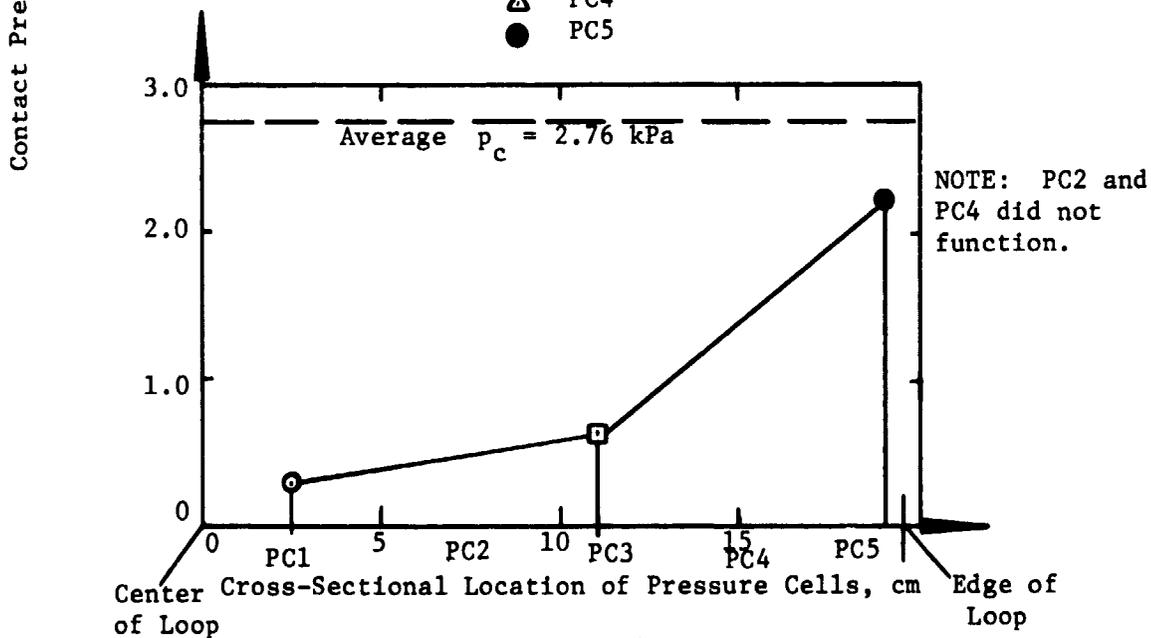
Evaluation of Contact Pressure Distribution

88. The results of two tests performed for the purpose of evaluating the distribution of contact pressures exerted by the ELMS are shown in figs. 28 and 29. For both tests, longitudinal sections along the direction of travel (figs. 28a and 29a) and cross sections perpendicular to the direction of travel (figs. 28b and 29b) were plotted. The trends of these plots elucidate the problems that were experienced with the pressure cells (paragraph 50); e.g. for 690-N load (fig. 28) none of the cells indicated a pressure higher than the expected average p_c . Although the data are incomplete for a quantitative analysis, the following qualitative conclusions can be drawn. In the longitudinal direction (figs. 28a and 29a), the maximum contact pressure appears to have occurred toward the middle of the contact length, indicating a relatively small amount of longitudinal loop stiffness. In contrast to this, the distributions perpendicular to the direction of travel show pressure concentrations at the edge of the loop (figs. 28b and 29b), indicating a relatively large amount of crosswise loop stiffness and mechanical behavior of the supporting soil similar to that of an elastic foundation.



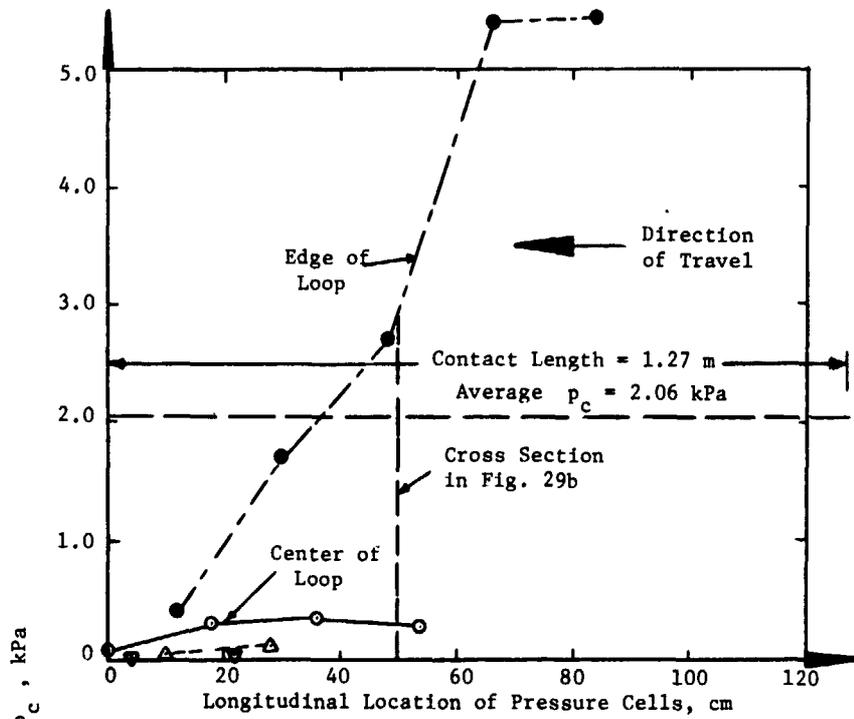
a. Longitudinal section
Pressure Cells (PC)

- PC1
- ▽ PC2
- PC3
- △ PC4
- PC5



b. Cross section

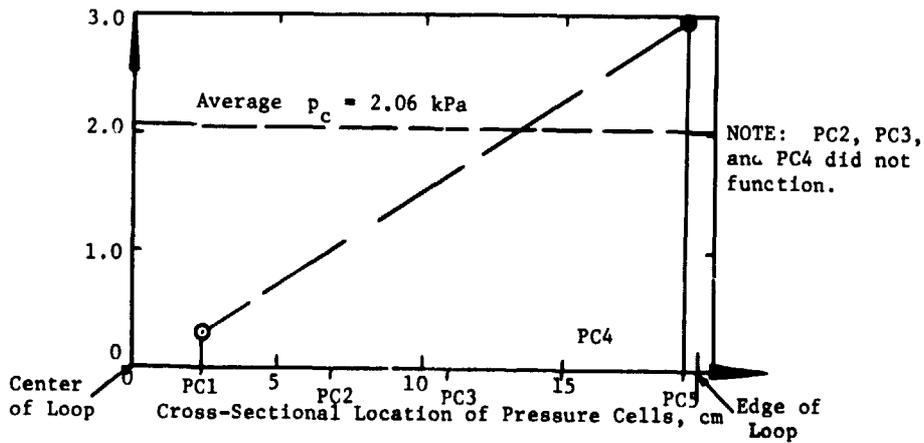
Fig. 28. Contact pressure distributions for ELMS II under 690-N load on soil condition LSS₁



a. Longitudinal section

Pressure Cells

- PC1
- ▽ PC2
- PC3
- △ PC4
- PC5



b. Cross section

Fig. 29. Contact pressure distributions for ELMS II under 565-N load on soil condition LSS₁

Comparison of ELMS II with Other Running Gears

89. Some of the performance characteristics of the ELMS II are compared in table 8 below with those of the following two running gears: the first-generation Elastic Loop Mobility System (ELMS I) developed by Lockheed (Melzer and Green, 1971) and the final version of the wheels for the U. S. Lunar Roving Vehicle (LRV) (wheel No. GM XIII in Green and Melzer, 1971).

Table 8

Running Gear	Pitch Condition	Soft-Soil Tests					α_{20}° deg	Maximum Step Obstacle Surmounted cm	Maximum Crevasse Crossed cm
		PC _T	PC ₂₀	PN _{SP}	PN ₂₀				
LRV	--	0.15*	0.26*	0.14*	0.52*	15*	[30]**	[70]**	
ELMS I	Free	0.18	0.33	0.15	0.54	18	--	--	
	Restrained	--	--	--	--	--	20	140	
ELMS II	Free	0.19	0.60	0.16	0.94	31	46	100	
	Restrained	0.12	0.68	0.11	1.02	34	38	100	

*Performance data of single LRV wheel.

**Performance data of 4x4 LRV vehicle (personal communication, Dr. Costes).

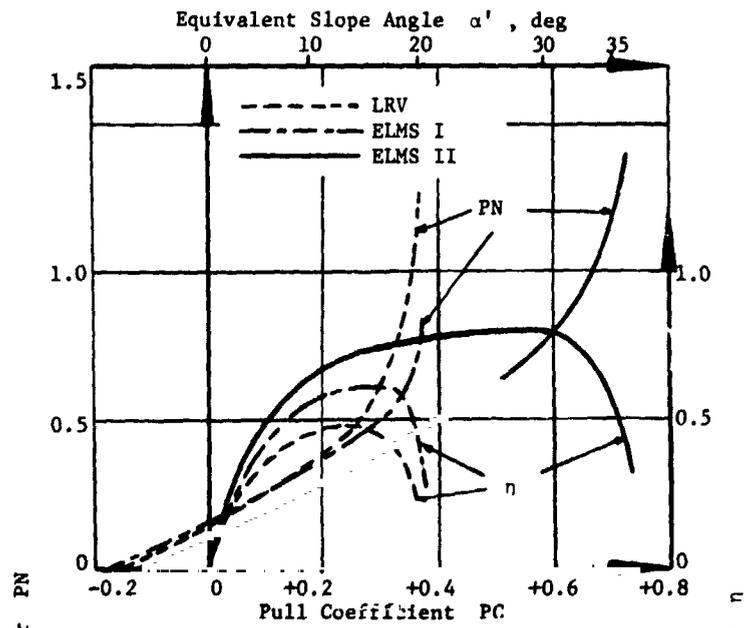
It should be pointed out that the soft-soil tests with the LRV wheel and the ELMS II were conducted on LSS₁, whereas the ELMS I was tested on a slightly firmer soil (LSS₄). However, based on the tabulation above, the ELMS II appears to be superior to the other two running gears in soft-soil performance, as well as in its performance in surmounting obstacles and crossing crevasses.

90. It should be pointed out also that the obstacle- and crevasse-negotiation capabilities of single ELMS (I or II) units cannot be compared with those of a 4x4 LRV vehicle, because the capabilities of a multiple-ELMS vehicle in negotiating obstacles or crevasses are expected to be far superior to those of a single ELMS unit. Obstacle- and crevasse-negotiation tests conducted with a 1/6-scale 3x3 ELMS II vehicle model, consisting of a

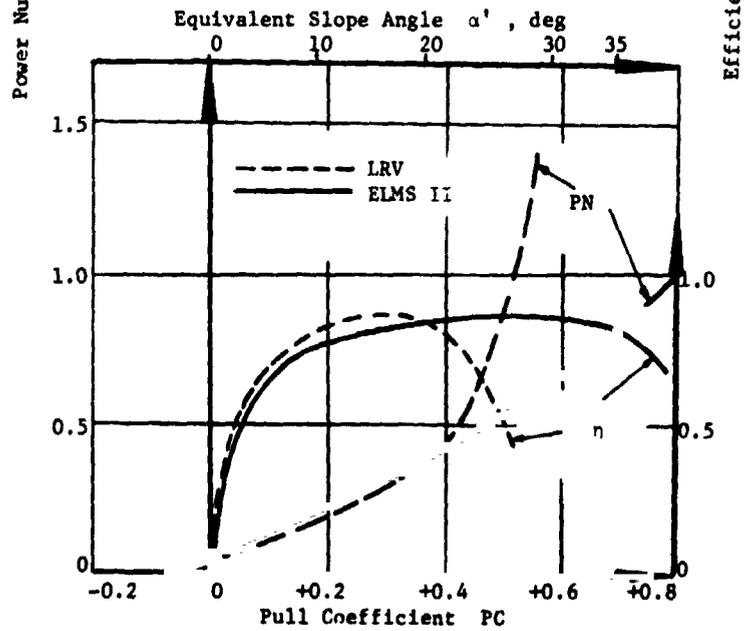
dual-ELMS II module with a "walking-beam" pitch-articulated suspension system and connected to a single ELMS II unit through adjustable pitch and yaw articulation (Costes, Melzer, and Trautwein, 1973), have indicated the following: (a) The maximum obstacle height by the ELMS vehicle model was achieved when the vehicle was operated in a free-pitch mode; this height was 85 percent of the ELMS length when the dual-ELMS II module was leading and 64 percent of the ELMS length when the single ELMS II unit was leading; (b) the maximum crevasse width negotiated was 90 percent of the ELMS length, which was achieved with the vehicle operated in a locked-pitch mode. Accordingly, the actual capabilities of powered multi-ELMS vehicles are expected to be far superior to those of single ELMS units listed in table 8. Nevertheless, even on the basis of the data shown in table 8, the performance of single ELMS units in negotiating obstacles or crevasses is indicated to be superior to that of a 4x4 LRV vehicle.

91. To complete the comparison, the power number and efficiency versus pull coefficient relations of the ELMS II in restrained-pitch mode on level ground (best operational condition) were compared with corresponding relations for the ELMS I and the LRV wheel (fig. 30). The most interesting observation that can be made here is that on loose soil (LSS_1), the ELMS II clearly outperformed the other two running gears (fig. 30a). However, on firm soil (LSS_5), the LRV wheel* was as efficient as the ELMS II for PC values smaller than about 0.4 (fig. 30b). This was not unexpected, because the better flotation characteristics of the ELMS II are not as necessary on firm soil as they are on loose soil, where, in fact, the ELMS II outperformed the LRV wheel. However, for PC values larger than about 0.4, the efficiency of the ELMS II was again larger than that of the LRV wheel. This means that the traction provided by the ELMS II at higher PC values is not only better than that of the LRV wheel, but also more efficient. Because of the large contact area, the ELMS II experienced less energy losses (e.g. sinkage) than the LRV wheel.

* Only the LRV wheel could be incorporated in the comparison on LSS_5 , because data with the ELMS I on LSS_5 were not available.



a. Loose lunar soil simulant



b. Dense lunar soil simulant

Fig. 30. Comparison of ELMS I, ELMS II, and LRV wheel performances on level ground

PART IV: CONCLUSIONS AND RECOMMENDATIONS

Conclusions

91. Based on the findings of this study, the following conclusions are drawn:

- a. Within the test load range (565 N to 690 N), the ELMS soft-soil performance appears to be independent of load (paragraph 62).
- b. Within the rpm range tested, the soft-soil performance of the ELMS was independent of drum rpm and loop translational speed (paragraph 63).
- c. The ELMS performance on soft soil was influenced by pitch mode. When the ELMS was mounted in the dynamometer (phase I on level ground), the system performed better (in terms of pull and slope-climbing capability) at a given input (in terms of power requirements) when it was operated under a restrained-pitch mode (paragraph 65). However, when the ELMS was connected to the trailer (phase II on slopes), the same trend developed only for pull coefficients smaller than 0.5. For larger pull coefficients, the energy required to achieve a certain output was larger in restrained-pitch mode than in the free-pitch (paragraph 75).
- d. Slope-climbing capability with the ELMS operating in a free-pitch mode can be predicted from single-unit tests on level ground and in free-pitch mode (paragraph 79). However, for a restrained-pitch mode, this is possible only for pull coefficients smaller than about 0.4, or slopes of about 22 deg (paragraph 80).
- e. The ELMS climbed the following maximum slopes: 35 deg in free-pitch mode on dense soil (LSS_5); 34 deg in restrained-pitch mode on dense soil; and 27 deg in the restrained-pitch mode on loose soil (LSS_1). Accounting for load transfer, which took place in the restrained-pitch mode, the corresponding maximum angles were 38 deg on LSS_5 (paragraph 74), and about 35 deg on LSS_1 (paragraph 78). This effect of load transfer could be avoided, if the trailer were replaced by a second powered ELMS II unit.

- f. Soil strength influenced ELMS performance. The energy required for a given system output was larger on loose soil than on dense (paragraphs 68 and 78). Soil strength also affected the maximum slope-climbing capability (see conclusion e above).
- g. The maximum rigid-step obstacle surmounted by the single ELMS II unit was 46 cm high, and the maximum crevasse crossed was 100 cm wide (paragraphs 83 and 84). In both cases, larger obstacles or crevasses could have been negotiated, if the trailer had been replaced by a second or a system of powered ELMS II units.
- h. For torque coefficients smaller than about 0.5 (corresponding to about 60 percent of the maximum available torque), the internal losses of the ELMS II were smaller than those of the first-generation ELMS (ELMS I). For larger torque coefficients, the internal losses of the ELMS I were smaller (paragraph 86).
- i. The ELMS II showed an overall superior performance to that of the ELMS I and the wheels used on the U. S. Lunar Roving Vehicle (paragraphs 89-91).

Recommendations

93. The following general recommendations are presented for consideration. Three or four model units should be built and tested to study the performance of the ELMS if used as a running gear for a vehicle. Special consideration should be given to the evaluation of the optimum ELMS configuration, i.e. three-looped or four-looped, and especially to the development of the pitch-control system in the linkage between units.

LITERATURE CITED

1. Costes, N. C., Farmer, J. E., and George, E. B., "Mobility Performance of the Lunar Roving Vehicle: Terrestrial Studies - Apollo 15 Results," NASA Technical Report No. F-401, 1972, National Aeronautics and Space Administration, Washington, D. C.
2. Costes, N. C. and Trautwein, W., "Elastic Loop Mobility System - A New Concept for Planetary Exploration," Journal of Terramechanics, Vol 10, No. 1, 1973, p 89.
3. Costes, N. C., Melzer, K.-J., and Trautwein, W., "Terrain-Vehicle Dynamic Interaction Studies of a Mobility Concept (ELMS) for Planetary Surface Exploration," AIAA Paper No. 73-407, 1973, presented at AIAA/ASME/SAE 14th Structures, Structural Dynamics, and Materials Conference, Williamsburg, Va., 20-22 Mar 1973.
4. Freitag, D. R., Green, A. J., and Melzer, K.-J., "Performance Evaluation of Wheels for Lunar Vehicles," Technical Report M-70-2, Mar 1970, U. S. Army Engineer Waterways Experiment Station, CE, Vicksburg, Miss.
5. Green, A. J. and Melzer, K.-J., "Performance of the Boeing-LRV Wheels in a Lunar Soil Simulant; Effect of Wheel Design and Soil," Technical Report M-71-10, Report 1, Dec 1971, U. S. Army Engineer Waterways Experiment Station, CE, Vicksburg, Miss.
6. Lessem, A. S., "Operations and Maintenance Manual for a Scale-Model Lunar Roving Vehicle," Miscellaneous Paper M-72-3, Apr 1972, U. S. Army Engineer Waterways Experiment Station, CE, Vicksburg, Miss.
7. Melzer, K.-J., "Performance of the Boeing LRV Wheels in a Lunar Soil Simulant; Effects of Speed, Wheel Load, and Soil," Technical Report M-71-10, Report 2, Dec 1971, U. S. Army Engineer Waterways Experiment Station, CE, Vicksburg, Miss.
8. Melzer, K.-J. and Green, A. J., "Performance Evaluation of a First-Generation Elastic Loop Mobility System," Technical Report M-71-1, May 1971, U. S. Army Engineer Waterways Experiment Station, CE, Vicksburg, Miss.
9. Melzer, K.-J. and Trautwein, W., "Performance Characteristics of a First-Generation Elastic Loop Mobility System," Proceedings, Fourth International Conference on Terrain-Vehicle Systems, Stockholm, 1972, Vol I, p 83.
10. Trautwein, W., "Design, Fabrication and Delivery of an Improved Single Elastic Loop Mobility System (ELMS)," Report HREC-7727-1 and HREC-7727-2, LMSC-HREC D 225600-1, 1972, Lockheed Missiles and Space Co., Huntsville, Ala.

APPENDIX A: DATA TABLES

Table A1

Soil Properties and Parameters, Before Traffic Data

	LSS ₁			LSS ₅				
	No. of Tests	Maxi- mum	Mini- mum	Aver- age	No. of Tests	Maxi- mum	Mini- mum	Aver- age
Penetration Resistance - Gradient, MPa/m	70	0.84	0.09	0.30	130	9.47	3.99	6.59
Dry Density, g/cm ³								
Gradient G	70	1.606	1.455	1.538	130	1.746	1.659	1.708
Gravimetric	12	1.728	1.618	1.685	38	1.880	1.600	1.742
Moisture Content, %								
Soil Bin	12	1.3	0.9	1.2	38	2.4	1.4	1.8
Surface	33	1.3	0.7	1.0	75	2.2	1.1	1.8
Relative Density, %								
Gradient G	70	45.0	21.0	34.0	130	64.0	52.0	59.0
Gravimetric	12	62.0	46.0	55.0	38	79.0	45.0	64.0
Shear Strength								
Friction Angle, deg	σ_s	-	-	38.8	-	-	-	41.5
Friction Angle, deg	σ_{pl}	-	-	34.2	-	-	-	36.0
Cohesion, kPa	c_{tr}	-	-	0.16	-	-	-	2.9

* $\sigma_n = 5.8$ kPa.** $\sigma_n = 7.3$ kPa.

Table A2
Soil Properties and Parameters, During-Traffic Data

Test No.	Soil	Pass No.	Penetration Resistance Gradient			Surface Moisture Content w, %			Dry Density γ_d , g/cm ³ (Gravimetric)			Moisture Content w, %		
			Max	Min	Avg	Max	Min	Avg	No. 1	No. 1	Avg	Reading No. 1	Reading No. 2	Avg
Tests on Level Ground (Phase I)														
A-72-001-6	LSS ₁	0	0.84	0.31	0.61	-	-	-	-	-	-	-	-	-
		0*	-	-	-	-	-	-	-	-	-	-	-	-
		1	0.95	0.75	0.85	-	-	-	-	-	-	-	-	-
-002-6	LSS ₁	2	2.83	0.64	1.24	-	-	-	-	-	-	-	-	-
		0	0.50	0.14	0.21	0.9	0.8	0.8	-	-	-	-	-	-
		0*	1.10	0.14	0.53	-	-	-	-	-	-	-	-	-
-005-6	LSS ₁	1	0.46	0.13	0.32	-	-	-	-	-	-	-	-	-
		2	0.60	0.33	0.48	-	-	-	-	-	-	-	-	-
		0	0.52	0.29	0.42	1.0	0.8	0.9	-	-	-	-	-	-
-006-6	LSS ₁	0*	0.60	0.06	0.38	-	-	-	-	-	-	-	-	-
		1	0.46	0.07	0.37	-	-	-	-	-	-	-	-	-
		2	0.58	0.33	0.44	-	-	-	-	-	-	-	-	-
-020-6	LSS ₅	0	0.72	0.32	0.45	-	-	-	-	-	-	-	-	-
		0*	-	-	-	-	-	-	-	-	-	-	-	-
		1	1.08	0.57	0.79	-	-	-	-	-	-	-	-	-
		2	-	-	-	-	-	-	-	-	-	-	-	-
		0	7.73	6.96	7.12	1.9	1.1	1.4	-	-	-	-	-	-
		0*	11.47	6.81	8.95	-	-	-	-	-	-	-	-	-
		1	8.02	5.45	6.91	-	-	-	-	-	-	-	-	-
		2	-	-	-	-	-	-	-	-	-	-	-	-

(Continued)

*Center line plus offset center line.

Table A2 (Continued)

Test No.	Soil	Pass No.	Penetration Resistance Gradient G, MPa/m			Surface Moisture Content w, %			Dry Density γ_d , g/cm ³ (Gravimetric)			Moisture Content w, %		
			Max	Min	Avg	Max	Min	Avg	Reading No. 1	Reading No. 2	Avg	Reading No. 1	Reading No. 2	Avg
Tests on Level Ground (Phase I) (Continued)														
A-72-021-6	LSS ₅	0	7.51	6.23	6.70	1.8	1.6	1.7	1.762	1.770	1.766	1.5	1.6	1.6
		0*	10.17	6.23	8.19	-	-	-	-	-	-	-	-	-
		1	8.06	5.18	6.96	-	-	-	-	-	-	-	-	-
		2	8.13	6.20	7.32	-	-	-	-	-	-	-	-	-
-022-6	LSS ₅	0	8.63	6.85	7.94	1.9	1.7	1.8	1.792	1.800	1.796	1.6	1.6	1.6
		0*	13.67	6.85	10.70	-	-	-	-	-	-	-	-	-
		1	8.20	7.17	7.55	-	-	-	-	-	-	-	-	-
-023-6	LSS ₅	0	8.43	7.16	7.90	1.9	1.5	1.7	1.676	1.680	1.678	1.8	2.1	2.0
		0*	13.08	7.16	9.66	-	-	-	-	-	-	-	-	-
		1	8.72	7.18	7.90	-	-	-	-	-	-	-	-	-
-024-6	LSS ₅	0	9.47	7.32	8.30	-	-	-	1.712	1.654	1.683	1.7	1.8	1.8
		0*	12.60	7.32	10.10	-	-	-	-	-	-	-	-	-
		1	9.90	7.84	8.35	-	-	-	-	-	-	-	-	-
-025-6	LSS ₅	2	9.06	7.43	8.14	-	-	-	-	-	-	-	-	-
		0	6.62	5.44	5.44	1.8	1.7	1.8	1.784	1.732	1.758	1.9	2.3	2.1
		0*	11.02	5.44	7.88	-	-	-	-	-	-	-	-	-
-026-6	LSS ₅	1	7.35	5.62	6.56	-	-	-	-	-	-	-	-	-
		0	7.04	5.34	6.13	2.0	1.7	1.9	1.711	1.749	1.730	1.6	1.6	1.6
		0*	10.02	5.34	8.25	-	-	-	-	-	-	-	-	-
		1	7.13	3.62	6.15	-	-	-	-	-	-	-	-	-
		2	7.75	6.34	6.96	-	-	-	-	-	-	-	-	-

(Continued)

Table A2 (Continued)

Test No.	Soil	Pass No.	Penetration Resistance Gradient		Surface Moisture Content w, %		Dry Density γ_d , g/cm ³ (Gravimetric)		Moisture Content w, %									
			Max	Min	Max	Min	Reading	Reading	Reading	Reading								
			G, MPa/m	MPa/m	MPa/m	MPa/m	No. 1	No. 2	No. 1	No. 2	Avg							
Tests on Level Ground (Phase I) (Continued)																		
A-72-027-6	LSS ₅	0	6.93	5.24	6.01	1.9	1.9	1.9	-	-	-	-	-	-	-	-	-	-
		0*	9.50	5.24	8.05	-	-	-	-	-	-	-	-	-	-	-	-	-
		1	7.22	6.18	6.77	-	-	-	-	-	-	-	-	-	-	-	-	-
		2	7.28	5.90	6.64	2.0	1.9	2.0	-	-	-	-	-	-	-	-	-	-
-028-6	LSS ₅	0	8.23	7.56	7.78	2.0	2.0	2.0	1.702	1.702	1.711	1.6	1.5	1.6	1.6	1.5	1.5	1.6
		0*	12.32	7.56	10.34	-	-	-	-	-	-	-	-	-	-	-	-	-
		1	9.04	7.65	8.22	-	-	-	-	-	-	-	-	-	-	-	-	-
		2	8.92	7.54	8.15	1.6	1.5	1.6	-	-	-	-	-	-	-	-	-	-
-029-6	LSS ₅	0	6.24	5.02	5.62	1.6	1.5	1.6	1.690	1.686	1.688	1.9	1.7	1.8	1.9	1.7	1.7	1.8
		0*	9.22	5.02	7.54	-	-	-	-	-	-	-	-	-	-	-	-	-
		1	6.68	5.97	6.30	-	-	-	-	-	-	-	-	-	-	-	-	-
		2	6.70	4.03	5.54	1.6	1.6	1.6	-	-	-	-	-	-	-	-	-	-
-030-6	LSS ₅	0	6.77	5.26	5.97	2.1	1.4	1.8	1.716	1.600	1.658	1.8	1.8	1.8	1.8	1.8	1.8	1.8
		0*	11.73	5.26	8.10	-	-	-	-	-	-	-	-	-	-	-	-	-
		1	7.37	5.66	6.63	-	-	-	-	-	-	-	-	-	-	-	-	-
		2	8.37	6.52	6.94	2.0	1.6	1.8	-	-	-	-	-	-	-	-	-	-
-031-6	LSS ₅	0	8.50	7.05	7.77	2.0	1.6	1.8	1.738	1.650	1.694	2.1	2.2	2.2	2.1	2.2	2.2	2.2
		0*	10.56	7.05	8.76	-	-	-	-	-	-	-	-	-	-	-	-	-
		1	8.94	7.44	8.07	-	-	-	-	-	-	-	-	-	-	-	-	-
		2	8.20	6.94	7.93	-	-	-	-	-	-	-	-	-	-	-	-	-
-032-6	LSS ₅	0	6.65	5.26	6.08	1.9	1.4	1.7	1.722	1.740	1.731	1.9	1.9	1.9	1.9	1.9	1.9	1.9
		0*	8.26	5.26	6.74	-	-	-	-	-	-	-	-	-	-	-	-	-
		1	7.09	5.55	6.45	-	-	-	-	-	-	-	-	-	-	-	-	-
		2	8.67	5.30	6.45	-	-	-	-	-	-	-	-	-	-	-	-	-

(Continued)

Table A2 (Continued)

Test No.	Soil	Pass No.	Penetration Resistance Gradient			Surface Moisture Content w, %			Dry Density γ_d , g/cm ³ (Gravimetric)			Moisture Content w, %			
			G, MPa/m	Max	Min	AVG	Max	Min	AVG	Reading No. 1	Reading No. 2	AVG	Reading No. 1	Reading No. 2	AVG
Tests on Level Ground (Phase I) (Continued)															
A-72-033-6	LSS ₅	0	7.16	5.97	6.62	1.9	1.8	1.9	-	-	-	-	-	-	-
		0*	7.94	5.97	7.12	-	-	-	-	-	-	-	-	-	-
		1	8.08	6.44	6.93	-	-	-	-	-	-	-	-	-	-
		2	8.57	6.34	7.27	-	-	-	-	-	-	-	-	-	-
-034-6	LSS ₅	0	7.52	5.87	6.59	2.2	1.9	2.1	-	-	-	-	-	-	-
		0*	9.22	5.87	7.63	-	-	-	-	-	-	-	-	-	-
		1	7.82	6.29	6.91	-	-	-	-	-	-	-	-	-	-
		2	9.03	5.75	6.94	1.7	1.5	1.6	-	-	-	-	-	-	-
-035-6	LSS ₅	0	5.63	3.99	4.66	1.8	1.7	1.8	-	-	-	-	-	-	-
		0*	9.34	3.99	6.90	-	-	-	-	-	-	-	-	-	-
		1	6.83	4.87	5.72	-	-	-	-	-	-	-	-	-	-
		2	9.26	4.83	6.10	1.7	1.6	1.7	-	-	-	-	-	-	-
-036-6	LSS ₅	0	6.92	5.98	6.55	1.9	1.8	1.9	-	-	-	-	-	-	-
		0*	10.45	5.98	7.63	-	-	-	-	-	-	-	-	-	-
		1	7.32	5.07	6.40	-	-	-	-	-	-	-	-	-	-
		2	8.02	5.40	6.13	1.6	-	1.6	-	-	-	-	-	-	-
-037-6	LSS ₅	0	8.03	6.09	7.11	1.6	1.5	1.6	-	-	-	-	-	-	-
		0*	12.80	6.09	9.07	-	-	-	-	-	-	-	-	-	-
		1	13.84	6.01	7.87	-	-	-	-	-	-	-	-	-	-
		2	11.02	4.84	6.77	1.7	1.6	1.7	-	-	-	-	-	-	-
-038-6	LSS ₁	0	0.44	0.08	0.16	1.1	0.9	1.0	1.610	1.678	1.644	1.3	1.3	1.3	1.3
		0*	0.95	0.01	0.40	-	-	-	-	-	-	-	-	-	-
		1	0.57	0.20	0.44	-	-	-	-	-	-	-	-	-	-
		2	1.51	0.46	0.81	-	-	-	-	-	-	-	-	-	-

(Continued)

Table A2 (Continued)

Test No.	Soil	Pass No.	Penetration Resistance Gradient			Surface Moisture Content w, %			Dry Density γ_d , g/cm ³ (Gravimetric)			Moisture Content w, %		
			G, MPa/m			Content w, %			Reading			Reading		
			Max	Min	Avg	Max	Min	Avg	No. 1	No. 2	Avg	No. 1	No. 2	Avg
Tests on Level Ground (Phase I) (Continued)														
A-72-040-6	LSS ₁	0	0.69	0.17	0.39	1.2	0.7	1.0	1.728	1.662	1.695	1.1	1.1	1.1
		0*	1.60	0.01	0.54	-	-	-	-	-	-	-	-	-
		1	0.85	0.57	0.72	1.0	0.9	0.9	-	-	-	-	-	-
-041-6	LSS ₁	0	0.46	0.06	0.23	1.1	0.9	1.0	-	-	-	-	-	-
		0*	0.69	0.06	0.35	-	-	-	-	-	-	-	-	-
		1	0.56	0.08	0.38	-	-	-	-	-	-	-	-	-
-042-6	LSS ₁	0	0.53	0.25	0.39	1.1	0.9	1.0	1.704	1.722	1.713	1.1	1.1	1.1
		0*	1.28	0.21	0.38	-	-	-	-	-	-	-	-	-
		1	0.46	0.16	0.27	-	-	-	-	-	-	-	-	-
-043-6	LSS ₁	0	0.60	0.07	0.26	1.0	0.8	0.9	1.708	1.672	1.690	1.0	1.0	1.0
		0*	0.80	0.01	0.33	-	-	-	-	-	-	-	-	-
		1	0.67	0.01	0.18	-	-	-	-	-	-	-	-	-
-044-6	LSS ₁	0	0.52	0.01	0.19	1.1	1.0	1.1	-	-	-	-	-	-
		0*	1.17	0.01	0.42	-	-	-	-	-	-	-	-	-
-045-6	LSS ₁	0	0.45	0.02	0.24	1.1	0.9	1.0	-	-	-	-	-	-
		0*	0.91	0.02	0.46	-	-	-	-	-	-	-	-	-
		1	0.63	0.04	0.40	-	-	-	-	-	-	-	-	-
-046-6	LSS ₁	0	0.32	0.01	0.09	0.9	0.7	0.8	1.712	1.718	1.715	1.0	1.0	1.0
		0*	1.25	0.01	0.41	-	-	-	-	-	-	-	-	-
		1	0.49	0.01	0.07	-	-	-	-	-	-	-	-	-

(Continued)

Table A2 (Concluded)

Test No.	Soil	Pass No.	Penetration Resistance Gradient			Surface Moisture Content w, %			Dry Density γ_d , g/cm ³ (Gravimetric)			Moisture Content w, %		
			Max	Min	Avg	Max	Min	Avg	Reading No. 1	Reading No. 2	Avg	Reading No. 1	Reading No. 2	Avg
Tests on Slopes (Phase II)														
A-72-009-6	LSS ₅	0	8.70	4.90	6.70	1.6	1.4	1.5	1.730	1.790	1.760	1.9	1.7	1.8
		0*	8.90	4.90	6.95	-	-	-	-	-	-	-	-	-
		8	6.70	5.10	5.70	1.8	1.7	1.7	-	-	-	-	-	-
-012-6	LSS ₅	0	7.00	5.17	6.61	1.9	1.4	1.7	1.806	1.772	1.789	1.6	1.9	1.8
		0*	9.83	5.17	7.80	-	-	-	-	-	-	-	-	-
		7	10.20	6.71	8.60	-	-	-	-	-	-	-	-	-
-013-6	LSS ₅	0	6.70	5.30	6.10	1.9	1.5	1.7	1.850	1.880	1.865	1.6	1.5	1.6
		0*	9.98	4.38	3.12	-	-	-	-	-	-	-	-	-
		4	5.56	3.06	4.80	1.5	1.4	1.5	-	-	-	-	-	-
-014-6	LSS ₅	0	7.56	5.66	6.67	1.9	1.7	1.8	1.776	1.708	1.742	2.4	2.4	2.4
		0*	8.72	5.66	7.54	-	-	-	-	-	-	-	-	-
		5	7.49	5.44	6.21	-	-	-	-	-	-	-	-	-
-015-6	LSS ₅	0	6.60	5.80	6.42	2.2	2.1	2.2	1.716	1.702	1.709	2.3	2.3	2.3
		0*	9.39	5.80	7.78	-	-	-	-	-	-	-	-	-
		8	8.09	6.14	7.18	2.4	2.1	2.3	-	-	-	-	-	-
-016-6	LSS ₅	0	7.60	4.96	5.87	2.1	2.0	2.1	1.738	1.698	1.718	2.3	2.3	2.3
		0*	10.86	4.93	7.25	-	-	-	-	-	-	-	-	-
		3	8.01	6.05	6.90	2.4	2.2	2.3	-	-	-	-	-	-
-017-6	LSS ₅	0	9.29	5.23	6.67	1.6	1.5	1.6	1.802	1.794	1.798	1.8	1.4	1.6
		0*	9.84	5.23	7.98	-	-	-	-	-	-	-	-	-
		6	9.37	4.98	6.30	1.6	1.4	1.5	-	-	-	-	-	-
-018-6	LSS ₅	0	6.25	5.60	5.93	1.8	1.7	1.7	1.866	1.792	1.829	1.7	1.9	1.8
		0*	8.60	5.58	6.62	-	-	-	-	-	-	-	-	-
		2	5.56	4.80	5.21	2.0	1.7	1.8	-	-	-	-	-	-

Table A3

Results from Single Unit Tests, Constant-Slip Test Technique (Phase I)

Test No.	Pass	Penetration	Pitch Angle	Pitch Cont.	EWS rpm	Carriage Speed	Effective Wire Speed	Slip	P ₁	P ₂	P ₃	Torque (Strain-gage)	Torque (Current)	N ₁ /N ₂	N ₃ /N ₂	Power Number	Efficiency	Sink age	Pitch Moment	Iron Shock Absorber		Rear Shock Absorber				
																				Displacement	F ₁ /N	Displacement	F ₂ /N	Displacement	F ₃ /N	
1	1	1	+3	PR*	34.1	0.524	0.131	0.541	+3.1	+63	+0.54	+62	+0.62	52	+0.52	0.64	0.85	0.1	0	0.005	+3	0	0.023	-382	-8.8	
2	1	1	+5	PR*	29.9	0.468	0.131	0.471	+0.6	+72	+0.54	+84	+0.83	68	+0.68	0.83	0.58	0.0	0	0.007	+4	0	0.022	390	-8.6	
3	1	1	+6	PR*	30.5	0.427	0.131	0.483	+11.6	+84	+0.72	+84	+0.83	67	+0.67	0.95	0.76	0.1	0	0.005	+4	0	0.026	-588	-15.3	
4	1	1	+2	PR*	37.5	0.599	0.131	0.593	-1.0	+92	+0.29	+47	+0.47	35	+0.35	0.47	0.63	0.0	0	0.002	+9	0	0.019	-177	-3.4	
5	1	1	+5	PR*	25.1	0.360	0.131	0.397	+9.3	+80	+0.62	+80	+0.81	65	+0.65	0.89	0.70	0.0	0	0.004	+7	0	0.027	-509	-13.7	
6	1	1	+2	PR*	131.0	2.129	0.151	2.070	-2.9	+180	+0.25	-17	+0.16	-	-	-	-	-	0.1	0	0.027	+1	0	0.000	-9	0.0
7	1	1	+5	PR*	95.4	1.662	0.131	1.510	+1.2	+352	+0.51	+73	+0.70	64	+0.64	0.72	0.71	0.1	0	0.004	+13	0	0.020	-427	-8.6	
8	1	1	+4	PR*	101.2	1.596	0.131	1.603	+0.6	+365	+0.51	+65	+0.60	56	+0.56	0.60	0.83	0.0	0	0.009	+1	0	0.019	-370	-7.0	
9	1	1	+6	PR*	41.9	0.683	0.132	0.620	-10.2	-156	-0.29	-9	+0.11	-	-	-	-	-	0.2	0	0.038	-167	-6.4	0.001	+2	0.0
10	1	1	+8	PR*	31.9	0.385	0.132	0.310	+24.6	+411	+0.75	+83	+1.01	61	+0.61	1.32	0.56	0.1	0	0.001	+3	0	0.020	-384	-11.2	
11	1	1	+6	PR*	35.7	0.547	0.132	0.570	+4.0	+248	+0.45	+50	+0.59	38	+0.45	0.61	0.73	0.0	0	0.005	+7	0	0.015	-309	-4.1	
12	1	1	+8	PR*	32.2	0.433	0.132	0.515	+15.9	+394	+0.70	+78	+0.92	62	+0.73	1.09	0.54	0.0	0	0.007	+4	0	0.020	-568	-11.4	
13	1	1	+5	PR*	61.2	0.663	0.132	0.657	-0.9	-126	-0.23	-13	+0.16	-	-	-	-	-	0.1	0	0.033	-128	-4.2	0.001	+1	0.0
14	1	1	+1	PR*	38.6	0.616	0.132	0.616	0.0	-12	-0.02	+4	+0.05	6	+0.07	0.05	0.70	0.0	0	0.013	+8	0	0.000	-13	0.0	
15	1	1	+6	PR*	34.5	0.528	0.132	0.552	+4.3	+293	+0.53	+62	+0.73	44	+0.52	0.76	0.70	0.1	0	0.011	+11	0	0.016	-385	-6.2	
16	1	1	+3	PR*	124.6	3.046	0.167	1.930	-6.6	-167	-0.30	-17	+0.21	-	-	-	-	-	0.0	0	0.029	-244	-7.1	0.001	+31	0.0
17	1	1	+10	PR*	31.2	0.690	0.167	0.788	+7.8	+428	+0.74	+70	+0.82	63	+0.74	1.32	0.56	0.1	0	0.009	+21	0	0.018	-556	-10.0	
18	1	1	+7	PR*	108.4	1.658	0.167	1.670	+0.7	+232	+0.40	+40	+0.47	37	+0.44	0.47	0.85	0.0	0	0.013	+23	0	0.011	-266	-2.9	
19	1	1	+8	PR*	102.5	1.526	0.167	1.580	+3.4	+363	+0.62	+57	+0.64	55	+0.64	0.69	0.94	0.0	0	0.012	+23	0	0.015	-413	-6.2	
20	1	1	+10	PR*	85.0	0.888	0.167	1.310	+32.2	+443	+0.76	+73	+0.85	63	+0.73	1.25	0.61	0.0	0	0.010	+22	0	0.017	-531	-9.0	
21	1	1	0	PR*	34.4	0.546	0.130	0.540	-1.1	-72	-0.10	+7	+0.05	-	-	-	-	-	0.1	+32	-	-	0.006	+1	0.0	
22	1	1	0	PR*	39.3	0.637	0.130	0.618	-3.1	-174	-0.25	-6	-0.06	-	-	-	-	-	0.1	+59	-	-	0.003	+1	0.0	
23	1	1	0	PR*	22.1	0.330	0.130	0.348	+5.2	+422	+0.60	+93	+0.88	51	+0.48	0.93	0.65	0.0	0	0.011	-101	0	0.023	-681	-11.0	
24	1	1	0	PR*	29.5	0.412	0.130	0.454	+9.3	+285	+0.39	+71	+0.70	50	+0.49	0.79	0.51	0.2	0	0.013	+8	0	0.018	-300	-5.0	
25	1	1	0	PR*	122.2	2.000	0.130	1.925	-1.9	-122	-0.18	-10	-0.10	-	-	-	-	-	0.3	+38	-	-	0.002	+2	0.0	
26	1	1	0	PR*	127.3	2.069	0.130	2.000	-3.5	-220	-0.37	-22	-0.21	-	-	-	-	-	0.0	+65	-	-	0.003	+2	0.0	
27	1	1	0	PR*	82.1	1.733	0.130	1.790	+4.7	+418	+0.61	+72	+0.70	63	+0.61	0.73	0.83	0.0	0	0.010	-107	0	0.023	-496	-11.4	
28	1	1	0	PR*	38.2	0.619	0.149	0.596	-3.9	-176	-0.30	-18	-0.21	-	-	-	-	-	0.1	+65	-	-	0.003	+2	0.0	
29	1	1	0	PR*	37.1	0.596	0.149	0.579	-2.9	-169	-0.29	-17	-0.20	-	-	-	-	-	0.4	+67	-	-	0.003	0	0.0	
30	1	1	0	PR*	28.0	0.405	0.149	0.416	+7.1	+192	+0.68	+65	+0.76	55	+0.64	0.82	0.83	0.0	0	0.012	-126	0	0.017	-447	-7.6	
31	1	1	0	PR*	24.9	0.323	0.149	0.420	+23.1	+437	+0.75	+67	+0.77	63	+0.72	0.99	0.75	0.1	0	0.011	-141	0	0.018	-522	-9.4	
32	1	1	0	PR*	126.3	2.082	0.155	2.050	-1.6	-238	-0.42	-28	-0.32	-	-	-	-	-	0.0	+79	-	-	0.004	+8	0.0	
33	1	1	0	PR*	99.1	1.572	0.155	1.610	+2.6	+280	+0.51	+49	+0.55	42	+0.47	0.56	0.80	0.0	0	0.012	-102	0	0.015	-673	-7.1	
34	1	1	0	PR*	84.5	1.256	0.155	1.371	+6.3	+408	+0.71	+65	+0.73	59	+0.66	0.80	0.89	0.0	0	0.011	-136	0	0.018	-620	-11.1	
35	1	1	0	PR*	75.0	1.082	0.155	1.219	+11.2	+440	+0.77	+75	+0.84	60	+0.67	0.95	0.81	0.2	0	0.013	-135	0	0.019	-630	-12.0	
36	1	1	44	PR*	132.2	1.140	0.153	1.220	-0.9	-256	-0.35	-25	-0.23	-	-	-	-	-	0.0	+73	-	-	0.006	+66	0.0	
37	1	1	44	PR*	84.8	1.072	0.153	1.035	+3.0	+293	+0.39	+43	+0.60	61	+0.60	0.63	0.83	0.0	0	0.010	-64	0	0.020	-466	-8.4	
38	1	1	44	PR*	96.9	1.342	0.153	1.531	+0.6	+268	+0.39	+48	+0.46	44	+0.42	0.46	0.84	0.0	0	0.008	-62	0	0.020	-283	-5.7	
39	1	1	44	PR*	36.5	0.590	0.153	0.584	-1.0	-183	-0.32	-16	-0.18	-	-	-	-	-	0.0	+80	-	-	0.007	+1	0.0	
40	1	1	44	PR*	29.0	0.433	0.153	0.464	+6.7	+362	+0.63	+61	+0.69	55	+0.62	0.74	0.85	0.1	0	0.011	-102	0	0.018	-459	-8.3	
41	1	1	44	PR*	27.1	0.318	0.153	0.536	+22.1	+421	+0.73	+67	+0.76	63	+0.72	0.98	0.75	0.0	0	0.010	-117	0	0.020	-533	-10	
42	1	1	44	PR*	38.2	0.615	0.153	0.610	-0.8	-202	-0.34	-21	-0.23	-	-	-	-	-	0.1	+82	-	-	0.006	+2	0.0	
43	1	1	44	PR*	29.6	0.459	0.153	0.474	+3.2	+309	+0.53	+53	+0.57	47	+0.52	0.59	0.90	0.1	0	0.011	-109	0	0.018	-420	-7.0	
44	1	1	44	PR*	28.6	0.419	0.153	0.457	+8.3	+379	+0.65	+61	+0.68	58	+0.65	0.75	0.88	0.1	0	0.010	-127	0	0.020	-533	-10	

Soil Condition ISS

PR = PULL PROBABLY
 * = TEST PASSED
 ** = PULL PROBABLY



Table A3 (Concluded)

Stat. No.	Penetration Re- sistance Vo, $\frac{L}{D} \frac{D^2}{E}$	Pitch Angle Coast- down $\frac{L}{D}$ deg	EIMS rpm	Effective Speed Loop Radius V_e, m $\frac{m}{sec}$	Slip Z	Full P N	P/N	Torque (Strain- gage) $V_s, m-N$	Torque (Cur- rent) $V_c, m-N$	Torque M/C $\frac{M}{C}$	Power Number FN	Efficiency age	Sink- age Z, cm	Pitch Moment $M_p, m-N$	Front Shock Absorber		Rear Shock Absorber		
															Displacement f, m	Force F, N	Displacement f, m	Force F, N	
0-4-1	7.11	0-01	FR	64	123.6	2.044	0.153	1.978	-1.3	243	-0.40	-0.30	-0.30	-0.30	-0.87	-	-	0.007	+0.2
0-4-2	7.17	0-01	FR	44	81.8	1.189	0.153	1.341	+11.3	+612	+0.70	+0.76	60	0.84	-0.14	-	-	0.020	-642
0-4-3	7.27	0-01	FR	44	91.8	1.401	0.153	1.470	+4.7	+377	+0.64	+0.69	54	0.88	-0.107	-	-	0.019	-598
0-4-4	7.34	0-01	FR	44	73.4	1.027	0.153	1.172	+12.4	+418	+0.71	+0.68	61	0.81	-0.116	-	-	0.020	-667
0-4-5	7.41	0-01	FR	-3	41.1	0.660	0.149	0.645	-2.3	-175	-0.30	-0.27	-	-	+0.1	-	-	0.001	+22
0-4-6	7.47	0-01	FR	-3	31.5	0.417	0.149	0.456	-4.7	-148	-0.35	-0.32	57	0.81	-0.136	-	-	0.017	-655
0-4-7	7.54	0-01	FR	-3	29.0	0.417	0.149	0.456	-4.7	-148	-0.35	-0.32	57	0.88	-0.136	-	-	0.017	-655
0-4-8	7.61	0-01	FR	-3	27.7	0.337	0.149	0.434	+22.4	+447	+0.76	+0.71	62	0.76	-0.146	-	-	0.018	-511
0-4-9	7.68	0-01	FR	-3	126.1	2.058	0.154	2.040	-0.9	-145	-0.25	-0.25	-	-	+0.1	-	-	0.001	+19
0-4-10	7.75	0-01	FR	-3	102.7	1.565	0.154	1.655	+5.4	+371	+0.75	+0.67	52	0.89	-0.107	-	-	0.015	-466
0-4-11	7.82	0-01	FR	-3	70.3	0.996	0.134	1.131	+11.9	+443	+0.86	+0.77	61	0.82	-0.126	-	-	0.016	-549
0-4-12	7.89	0-01	FR	-3	36.1	0.605	0.155	0.585	-3.4	-140	-0.24	-0.24	-	-	-	-	-	0.000	+10
0-4-13	7.96	0-01	FR	-2	35.7	0.580	0.155	0.571	-1.6	-110	-0.19	-0.19	-	-	-	-	-	0.000	+10
0-4-14	8.03	0-01	FR	+5	31.5	0.480	0.155	0.511	+6.1	+197	+0.34	+0.37	34	0.86	-	-	-	0.010	-273
0-4-15	8.10	0-01	FR	+7	30.9	0.447	0.155	0.501	+10.8	+239	+0.41	+0.49	39	0.81	-	-	-	0.000	+30
0-4-16	8.17	0-01	FR	+9	29.0	0.363	0.155	0.471	+23.0	+384	+0.65	+0.72	59	0.70	-	-	-	0.001	+24
0-4-17	8.24	0-01	FR	0	35.0	0.557	0.151	0.555	-0.4	-43	-0.0	+0.05	1	-	0.7	-	-	0.002	+6
0-4-18	8.31	0-01	FR	0	28.9	0.412	0.151	0.458	+10.0	+392	+0.56	+0.59	62	0.70	-0.106	-	-	0.022	-543
0-4-19	8.38	0-01	FR	0	31.0	0.471	0.151	0.481	+2.1	+188	+0.27	+0.40	34	0.66	-0.122	-	-	0.012	-381
0-4-20	8.45	0-01	FR	0	23.2	0.327	0.151	0.368	+11.1	+418	+0.60	+0.71	51	0.75	-0.110	-	-	0.021	-684
0-4-21	8.52	0-01	FR	0	36.0	0.604	0.155	0.569	-5.8	-158	-0.27	-0.19	-	-	0.6	-	-	0.003	+81
0-4-22	8.59	0-01	FR	0	29.1	0.372	0.155	0.473	+21.4	+387	+0.65	+0.67	56	0.76	-0.103	-	-	0.018	-514
0-4-23	8.66	0-01	FR	0	21.1	0.432	0.155	0.506	+14.6	+299	+0.45	+0.51	38	0.60	-0.103	-	-	0.016	-408
0-4-24	8.73	0-01	FR	0	35.4	0.483	0.155	0.511	+5.5	+243	+0.42	+0.52	35	0.76	-0.103	-	-	0.014	-388
0-4-25	8.80	0-01	FR	+4	35.5	0.586	0.155	0.575	-1.9	-184	-0.32	-0.16	-	-	0.5	-	-	0.005	+3
0-4-26	8.87	0-01	FR	+4	35.5	0.579	0.155	0.575	-0.7	-175	-0.30	-0.16	-	-	0.1	-	-	0.005	+8
0-4-27	8.94	0-01	FR	+4	28.8	0.385	0.155	0.466	+17.4	+384	+0.68	+0.76	58	0.74	-0.116	-	-	0.019	-640
0-4-28	9.01	0-01	FR	+4	30.6	0.458	0.155	0.496	+7.6	+261	+0.46	+0.55	41	0.77	-0.102	-	-	0.018	-543
0-4-29	9.08	0-01	FR	+4	29.3	0.443	0.155	0.475	+13.0	+357	+0.63	+0.71	56	0.82	-0.122	-	-	0.021	-670

Soil Condition LSS

FOLDOUT FRAME

1

Results of Foldout Tests (Sheet 11)

Test No.	Pass No.	Penetration Resistance Gradient MPa/m	Actual Slope Angle deg	Stabilized Load kN	Pitch Condition	ELMS mm	Actual Speed m/sec	Effective Loop Radius m	ELMS Speed m/sec	Full Calculation						PC = P _u /N	Loop (Strain-Axis) M _u , m-N	T _u = M _u /r, N	Torque (Current) N·m	Power Number PN	Pitch Force		Calculation of Load	
										P ₁ N	P ₂ N	P ₃ N	P ₄ N	P ₅ N	P ₆ N						Upper kN	Lower kN	Pitch Moment kN·m	Load Transfer kN
A-72-015-6	1	0	0	990	F	35.6	0.550	0.151	0.562	2.1	0	0	+11	+13	+0.02	22	0.21	7	0.22	+101	+232	0	-	
	2	0	0	990	F	35.1	0.540	0.151	0.555	2.1	0	0	+45	+45	+0.07	43	0.41	17	0.43	+83	+92	0	-	
	3	0	0	990	F	34.6	0.544	0.151	0.547	0.6	0	0	+68	+68	+0.10	40	0.37	17	0.47	+127	+601	0	-	
	4	0	0	990	F	34.3	0.543	0.151	0.542	0.7	0	0	+153	+153	+0.22	39	0.38	26	0.28	+183	+678	0	-	
	5	0	0	990	F	31.1	0.478	0.151	0.491	2.6	0	0	+150	+150	+0.44	57	0.59	54	0.51	+12	+587	0	-	
	6	0	0	990	F	barely go, P ₁ too large	-	-	-	-	0	0	+440	+440	+0.64	-	-	-	-	-	-	-	-	-
010-6	1	0	0	990	F	30.1	0.411	0.152	0.479	14.2	+195	+69	-69	+395	+0.70	66	0.77	53	0.90	+137	+675	0	-	
	2	0	0	990	F	30.6	0.237	0.149	0.478	10.5	+386	+67	-67	+386	+0.68	69	0.82	5	1.67	-201	+6.6	-75	70	
	3	0	0	990	F	30.1	0.362	0.152	0.479	24.4	+386	+67	-67	+386	+0.68	80	0.92	49	1.22	-285	+1365	-153	143	
011-6	1	0	0	990	F	34.5	0.501	0.150	0.541	-	0	0	0	0	0	10	0.10	5	-	-	-	-	-	
	2	0	0	990	F	32.9	0.501	0.150	0.517	3.1	0	0	0	0	0	5	0.05	4	1.05	-	-	-	(-20)	
	3	0	0	990	F	32.6	0.490	0.150	0.512	4.1	0	0	+278	+278	+0.40	42	0.51	49	0.53	-281	+457	-69	65	
	4	0	0	990	F	no go, P ₁ too large	-	-	-	-	0	0	+448	+448	+0.65	-	-	-	-	-	-	-	-	
	5	0	0	990	F	barely go, P ₁ too large	-	-	-	-	0	0	+419	+439	+0.64	-	-	-	-	-	-	-	-	
	6	0	0	990	F	27.3	0.392	0.150	0.428	8.4	0	0	+174	+174	+0.54	86	0.81	36	0.91	-363	+9.3	-42	86	
01-6	1	0	0	990	F	123.8	1.900	0.159	0.940	2.1	0	0	+14	+14	+0.02	9	0.09	63	0.09	-138	+81	-20	19	
	2	0	0	990	F	92.6	0.884	0.150	1.457	19.0	0	0	+363	+163	+0.53	58	0.56	64	0.93	-681	+786	-117	109	
	3	0	0	990	F	33.5	0.508	0.150	0.526	3.4	+120	+21	0	+141	+0.21	43	0.42	22	0.45	-231	+113	-51	48	
	4	0	0	990	F	33.7	0.516	0.150	0.530	2.7	+120	+21	+174	+315	+0.47	61	0.60	47	0.61	-409	+628	-98	92	
	5	0	0	990	F	30.3	0.141	0.150	0.473	7.3	+120	+21	+222	+363	+0.34	56	0.55	54	1.84	-554	+849	-133	122	
	6	0	0	990	F	29.5	0.312	0.150	0.464	32.6	+120	+21	+259	+400	+0.59	78	0.76	58	1.15	-505	+763	-118	110	
01-6	1	0	0	990	F	105.4	0.534	0.150	1.658	18.0	+120	+21	+264	+405	+0.60	68	0.67	68	1.08	-525	+1019	-144	115	
	2	0	0	990	F	35.1	0.533	0.149	0.548	7.2	+152	+60	50	+152	+0.59	54	0.51	38	1.63	-237	+283	-48	45	
	3	0	0	990	F	33.7	0.273	0.149	0.528	48.5	+152	+60	-40	+362	+0.61	59	0.67	52	1.29	-365	+559	-86	80	
	4	0	0	990	F	34.1	0.191	0.149	0.534	20	+366	+64	-64	+366	+0.63	72	0.83	51	2.30	-483	+580	-90	84	
014-6	1	0	0	990	F	31.9	0.263	0.149	0.498	47.2	+386	+67	-67	+386	+0.68	79	0.93	45	1.75	-311	+548	-89	75	
	2	0	0	990	F	35.1	0.516	0.150	0.551	6.4	+236	+41	+10	+287	+0.44	37	0.37	30	0.63	177	+7.7	-83	79	
	3	0	0	990	F	30.7	0.466	0.150	0.482	1.3	+236	+41	+72	+304	+0.54	65	0.67	50	0.69	-290	+711	-64	88	
	4	0	0	990	F	29.6	0.164	0.150	0.465	64.7	+236	+41	+146	+423	+0.65	64	0.66	36	0.87	-	-	-	(-120)	
	5	0	0	990	F	29.9	0.404	0.150	0.470	13.7	+236	+41	+101	+178	+0.58	66	0.68	54	0.79	-277	+727	-97	91	
	6	0	0	990	F	110.2	1.654	0.150	1.731	4.4	+236	+41	+20	+297	+0.46	54	0.55	64	0.58	-243	+907	-107	100	
01-6	1	0	0	990	F	35.0	0.536	0.150	0.553	3.1	+179	+11	0	+210	+0.31	49	0.49	37	0.50	-224	+863	-191	94	
	2	0	0	990	F	32.7	0.501	0.150	0.516	2.9	+179	+11	+55	+265	+0.40	49	0.49	37	0.50	-333	+348	-29	56	
	3	0	0	990	F	33.8	0.516	0.150	0.534	3.3	+179	+11	+110	+320	+0.48	62	0.62	42	0.64	-366	+483	-73	68	
	4	0	0	990	F	31.7	0.469	0.150	0.532	11.8	+179	+11	+145	+355	+0.53	4	0.64	50	0.72	-115	+537	-82	77	
	5	0	0	990	F	29.6	0.354	0.150	0.467	24.2	+179	+11	+204	+414	+0.62	63	0.73	36	0.83	-122	+738	-108	101	
	6	0	0	990	F	31.1	0.250	0.150	0.491	49.0	+179	+11	+231	+441	+0.66	77	0.77	57	1.51	-627	+813	-115	108	
01-6	1	0	0	990	F	31.6	0.442	0.150	0.500	11.6	+292	+51	+21	+355	+0.57	61	0.65	49	0.73	-505	+621	-105	99	
	2	0	0	990	F	30.0	0.149	0.150	0.475	68.6	+292	+51	+4	+417	+0.67	64	0.68	6	2.36	-43	+517	-89	86	

* Full barrel disturbed.
 ** If no steel
 † After last pass.
 ‡ Number in parenthesis indicates pitch moment that is not used.
 †† Elastically re-strained pitch.

Table A6
Results from Slope Tests; Acceptance Tests, Soil Condition LLS₁, Fully Restrained Pitch

Test No.	Pass No.	Penetration Resistance Gradient G, MPa/m	ELMS Speed m/sec	Actual Slope Angle α , deg	Minimum Torque			Maximum Torque			
					Slip %	Pull Coefficient PC = P/W _N	Torque Coefficient TC = M/W _N r _e *	Power Number PN	Slip %	Pull Coefficient PC = P/W _N	Torque Coefficient TC = M/W _N r _e *
A-72-007-6	1	0.18	0.5	0	0.5	-- **	(0.20)	--	32	-- **	(0.14)
	2	--	0.5	0	0.3	-- **	(0.07)	--	38	-- **	(0.21)
A-72-008-6	1	0.17	0.20-0.6	25	50.0	-- **	(0.43)	0.87	91	-- **	(0.50)
	2	--	0.5	25	29.0	0.57†	(0.47)	0.67	60	0.60†	(0.48)
A-72-009-6	1	0.27	0.20-0.6	28	←	No go	←	←	←	--	--
	2	--	0.30-0.2	27††	22.0	0.60	0.94	1.20	79	0.60	1.05

Load Transfer and Corresponding Minimum Torque

Test No.	Pass No.	Penetration Resistance Gradient G, MPa/m	ELMS Speed m/sec	Actual Slope Angle α , deg	Pitch Moment M _p , m-N	Load Transferred		W' = W _N - L	PC' = P/W _N	TC' = M/W _N r _e	α' max, deg
						L, N	L ₁ , N				
A-72-007-6	1	0.18	0.5	0	--	--	--	--	--	--	--
	2	--	0.5	0	--	--	--	--	--	--	--
A-72-008-6	1	0.17	0.20-0.6	25	--	--	--	--	--	--	--
	2	--	0.5	25	--	--	--	--	--	--	--
A-72-009-6	1	0.27	0.20-0.6	28	--	--	--	--	--	--	--
	2	--	0.30-0.2	27††	(88)‡	82	533	0.69	1.08	1.38	0.50

* Numeric in parentheses indicate torque measured by motor current; otherwise, torque was measured by strain gages.
 ** No valid pull measurement available because of saturation of strain-gaged tension rings.
 † Pull measured by string pay-out device.
 †† Maximum slope.
 ‡ From fig. 21.

Table A7

Results of Obstacle-Surmounting and
Crevasse-Crossing Tests

<u>Type of Test</u>	<u>Height of Step, Width of Crevasse cm</u>	<u>Pitch Condition</u>	<u>ELMS II rpm</u>	<u>Peak Torque m-N</u>	<u>Test Result</u>
Step-obstacle surmounting	30	FR	5	35	Go
	38	FR	5	42	Go
	46	F	5	44	Go
Crevasse- crossing	100	F	33	47	Go
	100	FR	33	55	Go
	150	FR	65	-	No go
	150	FR	97	-	No go

21) 7, 1974